Sensors & Diagnostics

CRITICAL REVIEW

View Article Online
View Journal | View Issue

Cite this: *Sens. Diagn.*, 2024, **3**, 504

Paper-based point of care diagnostics for cancer biomarkers

Prateek Bhardwaj, *[a] Bharti Arora, †[a] Survanshu Saxena, †[a] Subhasini Singh, †[a] Pranoti Palkar, [b] Jayant Sastri Goda *[b] and Rinti Banerjee [a]

Early detection of cancers is key to a better prognosis. Advanced proteomics and genomic detection techniques offer great specificity and sensitivity, however, delayed symptomatic detection, cost, and patient-incompliant sample procurement limit routine cancer diagnosis, thus affecting treatment opportunities and patient survival. The revolutionary impact of paper-based COVID-19 antigen home test kits highlighted the importance of affordable routine diagnosis in tackling pandemics. Therefore, inexpensive, user-friendly, and sensitive paper-based biosensors can prove to be a game changer in the management of cancer. Even though the fabrication of paper-based biosensors is easy and inexpensive, their compromised sensitivity requires significant improvement for effective diagnosis. This review comprehensively and systemically focuses on highlighting the impactful advancements that occurred over the past 10 years to improve the sensitivity at different levels of paper-based detection *i.e.* advancements in paper chemistry, assay type, detection technique, and signal enhancement. A detailed focus has also been provided on the impact of advanced nanomaterials (classified into inorganic, organic, and amalgamation of both) in enhancing analyte detection, signal amplification, signal transmission, and signal readout to develop point-of-care systems with fast interpretation, better reliability, specificity, biocompatibility, and low detection limits for the early paper-based detection of cancer. Moreover, a specific section on the types of samples employed for cancer detection, comprehensive tabulation of validated biosensors with clinical samples, their current challenges, and future prospects can help disseminate extensive information in driving the research forward in low-cost diagnosis of cancer.

Received 26th December 2023,
Accepted 22nd February 2024

DOI: 10.1039/d3sd00340j

rsc.li/sensors

1. Introduction

Limitations in detecting minute concentrations of cancer-specific biomarkers and their unexplored presence in some malignancies account for delayed cancer detection, a major factor that indirectly affects the prognosis and mortality.[1] Advancements in molecular detection with the advent of highly sensitive genomic and proteomic technologies minimized these limitations to an extent, but technique-associated cost along with the requirement of basic infrastructure and trained operators limits their affordability in resource-constrained conditions especially in developing countries.[2] Therefore, paper-based diagnostic technologies that can meet WHO's ASSURED (affordable, sensitive, specific, user-friendly, rapid and robust, equipment-free, and deliverable to end-user) criteria are required.[3] Such technologies majorly utilize two kinds of substrates like cellulose fibre (filter and chromatography paper) and nitrocellulose membrane (uniform pore size, 0.45 μm) for fabrication because of their porous nature with modifiable surface chemistry and optical properties.[3,4] Filter papers with pore sizes 20–25 μm are generally used due to their appropriate porosity, hydrophilicity, stiffness, and lateral fluid flow rate.[3,4] The utilization of inexpensive biodegradable substrates makes these point-of-care devices easily scalable and disposable. Multiple types of paper-based POCs have been developed over the years starting from the conventional dipstick and lateral flow tests (latex agglutination and radioimmunoassay) in the late 1950s to advanced microfluidic tests utilizing different detection approaches namely colorimetric, fluorometric, or electrochemical.[5] To overcome the limitations associated with the sensitivity and specificity of conventional paper-based POCs, novel biomaterial-based approaches are being

[a] *Nanomedicine Lab, Department of Biosciences and Bioengineering, Indian Institute of Technology Bombay, 400076, India. E-mail: prateekbhardwaj26@gmail.com*
[b] *Department of Radiation Oncology, Advanced Centre for Treatment Research and Education in Cancer, Navi Mumbai, & Homi Bhabha National Institute, Maharashtra, India. E-mail: jgoda@actrec.gov.in*
† All three authors have contributed equally to this article.

employed to modify the surface properties of the paper through biopolymer coatings, impregnation or surface functionalization of paper with different nanoparticles, or the use of nanoparticles as sensing molecules for signal amplification.[4] Over the past 5 years, a handful of review articles highlighted the importance of low-cost paper-based diagnostics in cancer detection with individual focus on either type of paper-based diagnostics, microfluidic-based analytical devices, or the role of nanomaterials in cancer detection, however, a systemic and comprehensive review highlighting the advancements at all the fronts of paper-based cancer detection is highly desirable to drive the research in this domain.[6–11]

This review exhaustively highlights the impactful technological advancements that occurred over the past decade at each step of biomarker detection starting from advancements in paper substrate chemistry, assay type, and detection technique, to advanced signal enhancement strategies exploited in developing extremely sensitive paper-based biosensors specifically for cancer detection. In assay type, this review comprises conventional dipstick assays to advanced 3D μPADs (microfluidic paper-based analytical devices), wherein the detection techniques comprise dot blot, advanced immunochromatography integrated with nucleic acid amplification technique, molecularly imprinted polymers, and conducting papers. Importantly, a detailed

Prateek Bhardwaj

Dr. Prateek Bhardwaj is a Postdoctoral Associate in the Department of Therapeutic Radiology at Yale University, USA. His current research focuses on developing personalized medicine for leukemia by understanding and exploiting the synthetic lethal interactions between the genes involved in DNA damage response. Dr. Bhardwaj received his Ph.D. in Nanomedicine and Master's in biotechnology from the Indian Institute of Technology Bombay, India, where he specialized in developing biomaterial-based theranostic nano-platforms and radiosensitizing hydrogels for cancer treatment. He has been granted patents and published several high-impact peer-reviewed articles in journals like Nanoscale, Journal of Controlled Release, Biomaterials, Acta Biomaterialia, and Biomacromolecules.

Bharti Arora

Bharti Arora is pursuing her Ph. D. at the Max Planck Institute for Multidisciplinary Sciences, Göttingen. She works on identifying and correlating protein biomarkers from tumour tissues with the colorectal cancer patient database. She uses a variety of light microscopy techniques, such as multiphoton, confocal, and lightsheet microscopy for detailed tissue analysis. Additionally, she uses MALDI imaging for precise protein distribution studies and high-resolution X-ray imaging with PETRA III (synchrotron) for in-depth 3D examinations. She completed her master's in Biomedical Engineering at the Indian Institute of Technology Bombay, where she developed a point-of-care detection kit for urinary tract infections using nanoparticle-based biosensors.

Survanshu Saxena

Survanshu Saxena is currently pursuing his Ph.D. Degree in the School of Biomedical Engineering, McMaster University, Canada. He received his M.Tech. Degree in Biomedical Engineering from the Indian Institute of Technology, Bombay. His research interests include biomaterials, nanoparticles/nanomaterials, and polymers for biosensing applications.

Subhasini Singh

Subhasini Singh is pursuing her Ph.D. from the Leipzig University, Germany, where she focuses on developing origami biosensors for targeting membrane-active pathogens. She is also a part of EXIST-Women led start-up program where she is working on a start-up idea for providing an artificial lipid model systems for studying membrane-target interactions in vitro. Subhasini obtained her Master's degree in the field of Biotechnology from St. Xavier's college, Mumbai. Later, she joined Nanomedicine Lab at Indian Institute of Technology, Bombay as Junior Research Fellow where she was primarily involved in developing point-of-care technologies for detecting anti-microbial resistant strains.

focus was imparted to the advanced nanomaterial-based detection and signal amplification strategies with a systematic description based on the use of different inorganic, organic, and hybrid nanomaterials. It also provides an exhaustive comparison of the devices used in detecting different cancer biomarkers from different clinical samples and underlines their challenges and future implications in cancer diagnosis.

2. Advancements in the substrate (paper) chemistry

Advancements in paper-based devices originate from making small alterations in the functionality of the substrate (paper) itself. Chitosan not only enhances the wet-strength of μPADs but also stabilizes the immobilized antibodies.[12] Hence, chitosan-treated nitrocellulose membrane can be a good substrate for chemiluminescence ELISA (CL-ELISA) on paper.[13] The poly(oligoethylene glycol methacrylate) (POEGMA) coating on paper makes it a protein repellent, thus reducing the output signal noise due to non-specific adsorption of proteins in any biological sample.[14] Further, nitrocellulose sheets can be coated with a hydrophobic layer of polycaprolactone (PCL) to reduce the flow rate.[15] The reduction in the fluid flow rate in paperfluidic chips increases target-probe binding, ultimately resulting in a strong signal and lower limit of detection. To automate the sequential steps employed in the lateral flow assays, a water-swellable polymer-based intermediate strip can be added to the LFA design to automatically release the secondary reagents in a timely manner.[16] The synthesis of porous 'hydrogel walls' on the nitrocellulose paper can facilitate the capture of detection probes as they flow through the assay.[17] Polymer-based biochips have been developed as superior substrates for the detection of HPV from gynecological swabs and biopsies from genital warts.[18,19]

3. Advancements in the type of paper-based assays

Paper as a substrate can be utilized in various ways to develop a variety of assays for the detection of a specific cancer biomarker in different kinds of biological samples. Significant progress from employing conventional assays like dipstick to more advanced microfluidic-based detection of cancer has been discussed below (refer to Fig. 1).

3.1 Dipstick test

This rapid diagnostic method involves the dipping of an ordinary paper strip in a patient's sample to determine the type of malignancy based on color change after enzyme-catalyzed reactions, which can be correlated with the color-coded chart for a semi-quantitative determination as shown in Fig. 1. Initially, it was established in the 1950s as one of the vital point-of-care tests for the detection of glucose in the urine, however, its user-friendliness has fascinated many researchers to explore its potential for the detection of numerous diseases including cancer.[20] A direct comparison of the dipstick test with an established immuno-fecal occult blood test (IFOBT) for the detection of transferrin (Tf) and fecal hemoglobin respectively in the fecal discharge of patients with colon cancer and premalignant lesions reflected its superiority over IFOBT with a specificity of 76.5% over 69% (IFOBT). The IFOBT test generally detects hemoglobin discharged in feces of colon cancer patients, but the fecal hemoglobin is more prone to lysis due to the effect of

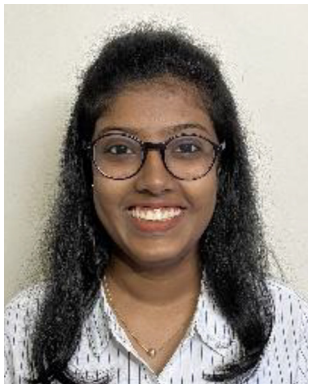

Pranoti Palkar

Pranoti Palkar pursued her Master's Degree in Pharmaceutical Biotechnology at DY. Patil University, Mumbai. Her master's dissertation research focused on nanomaterial-based dual-drug targeted delivery for effective glioblastoma therapy. In addition to her work in nanotechnology, Pranoti has keen interest in the field of radiation biology. Following the completion of her Master's, Pranoti joined ACTREC, Tata Memorial Centre, as Research Fellow in Department of Radiation Oncology. Driven by a desire to make real-world impact, Pranoti's research interest evolved to encompass the field of immunology. In the research lab, she leads the in vivo experiments on CAR-T cell therapy for treating multiple myeloma.

Jayant Sastri Goda

Dr. Jayant S Goda (MD, DNM, MRes) is a clinician scientist and Professor in Radiation Oncology at ACTREC, Tata Memorial Centre, Mumbai. As a translational researcher, his current focus is on testing novel compounds as radio-sensitizers and radioprotectors in mouse tumour xenografts, orthotopic and PDX models. He is actively pursuing research on novel drug delivery platforms using nanotechnology which is exemplified with the publications and patents in this area of research. As an academician and researchers, he has published more than 100 scientific articles in the field of clinical oncology and translational oncology in peer reviewed high impact journals.

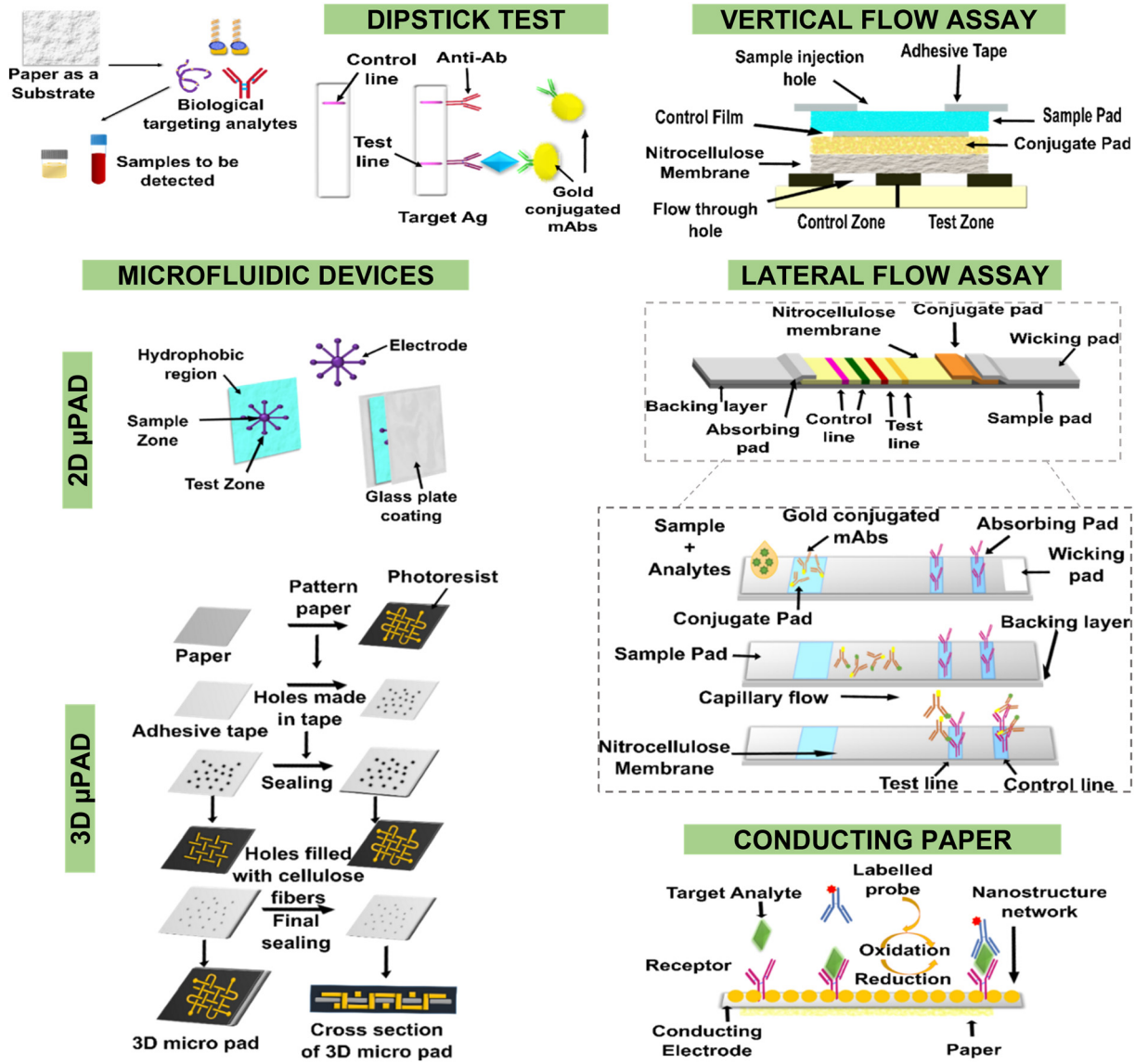

Fig. 1 Different types of paper-based biosensors.

bacteria or digestive enzymes.[21] Whereas, detection of transferrin discharged in feces due to bleeding by Tf dipstick test provides a more stable analysis as transferrin is resistant towards bacterial and digestive enzyme action.[22] Despite easy analysis and wide applicability of test strips, the use of dipstick assay is quite limited for cancer detection due to lack of precision, limited detection range, and requirement of large sample volume. Integration of paper strips with more advanced assays like flow-based and microfluidic-based significantly minimizes these limitations and has thus gained a lot of importance in cancer diagnosis.[23]

3.2 Flow assays

Flow assays have gained significant importance in the detection of various analytes in complex samples within a short period. They have been categorized into two main types *i.e.* lateral and vertical flow assays depending on the directionality of the flow of the sample due to capillary mode of action.

3.2.1 Lateral flow assay (LFA). LFA test strip consists of 4 major components – a sample pad, conjugate release pad, test pad, and an absorbent pad that are fixed on a backing card to ensure safe and proper handling as shown in Fig. 1. The sample pad facilitates the proper interactions of an analyte of interest with the molecules present on the conjugate pad and the nitrocellulose membrane. It also controls and maintains the flow rate of the sample with a homogenous distribution. The conjugate pad contains immobilized analyte-specific antibodies bound to colored or fluorescent particles and subsequently allows the release of conjugated molecules toward the test pad. Further, the membrane present between the conjugate pad and the test pad plays a key role in the interaction of conjugate molecules

with the target analyte and provides the surface for the interaction of conjugate molecules at the border of the test line and control line. The test line depicts the interaction through color change, which can be correlated to the concentration of the target analytes for qualitative, semi-quantitative, and quantitative analysis, whereas the control line depicts the positive capillary flow of the sample. The absorbent pad helps in maintaining the rate of capillary action and prevents the sample backflow.[24]

LFA is classified into two major formats; direct type and competitive type. Direct type can detect larger analytes and molecules with multiple antigenic sites in the form of the sandwich-based assay, whereas competitive type analyzes the smaller molecules with a single antigenic determinants.[25] Many LFA detection kits are available in the market for the detection of various cancers (refer to Table 1).

Though LFA offers advantages like easy detection, robustness, and specificity, its low reproducibility due to difficulty in controlling the sample flow rate, compromised user-friendliness owing to time-consuming sample pre-treatment, and cross-reactivity during multiplex LFA on a single strip leads to false positive errors. In addition,

Table 1 Commercially available LFA kits for cancer detection

Company	Product name	Cancer type	Analyte	Required sample	Detection time (min)	Sensitivity	Specificity	Ref.
CTK Biotech	On-site PSA semi-quantitative rapid test	Prostate	PSA	60–90 ml blood/ serum/plasma	10	100%	99%	26
	On-site FOB rapid test	Colorectal	hHB	Human fecal specimens	10	NR	NR	
Alere	Alere NMP22 BladderChek	Bladder	Nuclear matrix protein (NMP22)	4 drops of urine	30	99% when combined with cystoscopy	99% NPV along with cystoscopy	27
	Clearview iFOBT	Colon	Faecal occult blood	Faeces	5	93.60%	99.10%	
Arbor Vita Corp.	OncoE6 cervical test	Cervical	E6 oncoproteins	Cervical swab	150	84.6%	98.5%	28
	OncoE6™ oral test	Oral	E6 oncoproteins	NR	150	NR	NR	
Quicking Biotech Co., Ltd	CA125 rapid	Ovarian	CA125 Ag	100 μL of serum	5–10	40 U ml^{-1}	NR	29
Innovation Biotech	AFP test	Hepato-cellular	AFP	Serum plasma	10	25 ng ml^{-1}	NR	30
Diagnostic Automation/Cortez Diagnostics Inc.	CEA serum rapid test	Colon adenocarcinoma	CEA	Serum	10	5 ng ml^{-1}	NR	31
LifeSign, LLC	Status BTA	Bladder	Bladder tumor associated antigen	3 drops of urine	5	67%	70%	32
ALFA SCIENTIFIC DESIGNS	INSTANT-VIEW®	Prostate	PSA	Serum	4–7	4 ng ml^{-1}	NR	33
AccuBioTech Co., Ltd	AFP whole blood test cassette	Hepatocellular carcinoma	AFP	Blood/serum/ plasma	<10	99.3%	99.0%	34
	PSA whole blood test cassette	Prostate	PSA	Blood	<10	98.9%	98.6%	
	CEA whole blood test cassette	Hepato-cellular carcinoma	CEA	Blood	<10	98.7%	99.3%	
	FOB feces test strip	Colon	Human occult blood in feces	Blood	<10	94.6%	99.3%	
TÜRKLAB	CEA (carcino-embryonic antigen) test	Diagnosis of primary carcinomas	CEA	Blood/serum/ plasma	<10	99.3%	99.3%	35
	AFP (alpha fetal protein) test	Detection of many tumors at an earlier stage/detection of fetal open neural tube defects	AFP	Blood/serum/ plasma	<10	99.3%	99%	
	FOB (fecal occult blood) test	Colorectal cancer	Hb	Human faeces	<10	99.9%	97%	
Ulti med	FOB cassette	Colorectal cancer	Human occult blood	Human faeces	<10	NR	NR	36

NR: not reported.

processing of complex samples often requires sophisticated equipment which limits the use of such LFAs in hospitals and clinics thus affecting its overall operational flexibility and self-diagnosis at home.[37]

3.2.2 Vertical flow assay (VFA). VFA follows the same principle as LFA but differs in the direction of the flow of the sample, which is applied vertically in the presence of an external force.[37] Unlike LFA, VFA can minimize the concentration associated agglutination (Hooke's effect) of the analytes *e.g.*, antibodies and cross-reactivity issues associated with multiplexed detection of analytes.[37,38] Chen *et al.*, showed the multiplexed detection of prostate cancer-specific biomarkers *viz.* human alpha-fetoprotein (AFP), carcinoembryonic antigen (CEA) and prostate-specific antigen (PSA) in clinical serum samples using VFA with a sensitivity of up to picogram per millilitre.[39] Despite of likely applications of VFA, the use of antibody-conjugated gold colloids in conventional VFAs for visible red color analysis imparts drawbacks such as less precision and low sensitivity which can be significantly improved with the use of advanced sensing molecules discussed later in this review.[39]

3.3 Microfluidic paper-based analytical device (μPAD)

Paper-based microfluidics are point-of-care devices that consist of a set of hydrophilic cellulose fibres that direct the flow of liquid from the inlet to the outlet through permeation. The agglomerated cellulose fibres enhance the porosity of the device for the movement of the sample from the region of high concentration of analyte to the region of low concentration based on low Reynold's number *i.e.*, the ratio of inertial force to viscous force.[40] While fabricating the hydrophilic microfluidic paper, certain hydrophobic barriers are generated to restrict the flow of samples within the device to make it more sensitive and precise for detection.[41] It is a modified version of the standard lateral flow assay. The principle of paper-based microfluidics is the interaction of droplets of the sample with the cellulose fibres which ensures homogenous distribution by wetting the paper surface, followed by its wicking through the capillary mode of action.[42] There are three main types of microfluidic devices. Continuous microfluidic devices allow the continuous movement of samples in the presence of an external force through microporous channels by enhancing the liquid flow without any hindrance.[43] The second type is the droplet-based microfluidic device which comprises the motion of 2–3 fluids simultaneously creating droplets that are separated by an immiscible liquid within the micro-carrier channel. These devices have the advantage of generating highly reactive microreactor droplets due to a high surface-to-volume ratio, thus stimulating faster reactions, and performing multiple reactions in a device.[44] The third type is a new-generation digital microfluidic device that enables the movement of droplets on a series of planar electrodes. It is widely used due to its high scalability and minimum power utilization, along with a low sample requirement.[43] Fabrication of the microfluidic device determines its wettability and biocompatibility. Conventionally, glass and silicone were used for fabrication purposes followed by polymer-based compounds such as polydimethylsiloxane (PDMS) and polymethylmethacrylate (PMMA) to improve the tensile strength and wettability of the device, but paper-based microfluidics has emerged as one of the most promising diagnostic tool for several decades.[43] This technology was first established by Whitesides *et al.* in 2007 as an inexpensive and portable biosensor for the detection of glucose in urine.[43] Minimal sample requirement, controlled flow, low-cost fabrication, biocompatibility, stability, and robust capillary action are a few of its advantages.[45] In addition, various detection techniques (colorimetric, enzymatic, chemiluminescence, electrochemical) have also been miniaturized into a small chip for rapid analysis.[43] Microfluidic devices are found in either 2D or 3D format.

3.3.1 2D μPAD. 2D μPAD is similar to the lateral flow assay and follows the principle of capillary action in two dimensions. A 2D μPAD developed by Baynes *et al.* imparted the rapid detection (1 minute assay time) of colorectal cancer biomarkers *i.e.* CEA and carbohydrate antigen 19-9 (CA 19-9) in spiked human serum and blood samples with a detection limit of 1 pg ml^{-1} for CEA and 0.1 U ml^{-1} for CA 19-9.[46] It can also be used for the multiplexed detection of both biomarkers with negligible cross-reactivity and a sensitivity of 10 ng ml^{-1} for CEA and 50 U ml^{-1} for CA 19-9.[46] Major drawbacks of these devices in terms of large requirement of sample, inability to detect multiple samples with high sensitivity, and non-homogeneous sample distribution throughout the device led to their modification from 2-dimension to 3-dimension (3D μPAD).[47]

3.3.2 3D μPAD. 3D μPAD is the most advanced version of μPAD, which is equivalent to vertical flow assay and allows the movement of samples in all three dimensions. Thus, leading to high throughput screening, easy multiple sample detection, and homogenous distribution.[43] The 3D μPAD is fabricated by employing multiple layers of paper arranged in a systematic manner using double-sided tape with multiple holes occupied with hydrophilic material such as paper. This method is usually tedious and thus modified using hydrophilic adhesive sprays to glue the papers or cold lamination method, thus generating a rapid 3D μPAD device. However, one of the most widely used approaches is the use of the origami method by folding the paper into 3D stacks and holding it with pre-fabricated clamps.[48] Following fabrication, 3D μPADs are functionalized to enable the flow of samples in a regulated manner toward the detection zone for the analysis of results using detection meters.[20,49] Lee *et al.* showed the effectiveness of 3D μPAD impregnated with HRP conjugated anti-Trx-1 antibody for the detection of breast cancer by targeting thioredoxin-1 with the detection limit of 0–200 ng ml^{-1} in the blood serum samples within 14 min.[50] The high sensitivity and specificity of this technology have enabled its use for the detection of cancer-specific biomarkers in multiple samples within a short period, which can be further improved with continuous advancements in the detection techniques.

4. Advancements in detection techniques

Apart from using the paper in different ways for efficient cancer detection, significant improvement has occurred in functionalizing the surface of the paper for analyzing different types of cancer-specific biomarkers with enhanced sensitivity and specificity. Technologies employing the immobilization of antigen or antibodies for immune-based detection, integration of nucleic acid amplification for nucleic acid detection, and incorporation of advanced recognition elements and conducting layer onto the surface of the paper have been well described in this section (refer to Fig. 2).

4.1 Quantitative dot blot assay (QBD)

The identification of cancer biomarkers on a paper-based substrate started with the dot-immunoblot assays.[51] The antigen is blotted on the nitrocellulose sheet, which is further exposed to the primary antibody followed by a secondary antibody attached with an enzyme for colorimetric detection. (Fig. 2A) Alternatively, monoclonal antibodies were bound on paper discs.[52] Moving from 'enzyme-labeled' secondary antibodies, the fluorescently labeled secondary antibodies eliminated the 'enzymatic-reaction' step from the assay to identify tumour-associated proteins.[53] The dot-immunoblots were superseded by immuno-chromatographic assays (ICAs). A QDB assay can enhance the conventional immunoblot assay to achieve quantitative and high throughput analysis functionality. A QDB plate is engineered in a 96-well plate format with nitrocellulose paper as the binding surface on the base of each well (Fig. 2D). QDB has been used to study and quantify the profile of macrophage-capping protein (CAPG) from the prostate cancer tissue of TRAMP (transgenic adenocarcinoma of the mouse prostate) mice model.[54] The speed of the quantitative dot blot assay makes it an ideal option for situations where rapid results

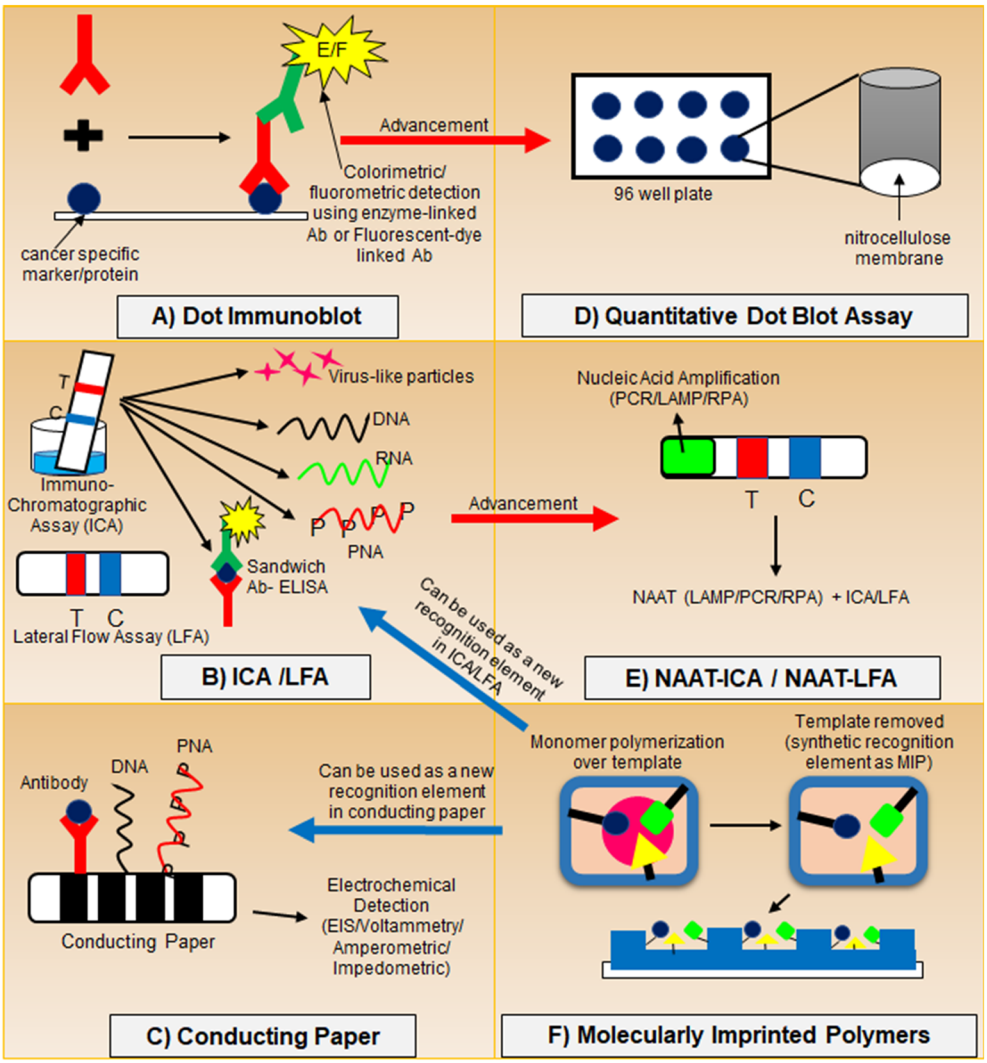

Fig. 2 Different mechanisms for the detection of analyte for paper-based diagnosis.

are required. The dot blot assays do not require time-consuming steps, *e.g.*, gel electrophoresis or several washes, compared to methods like Western blotting or ELISA. Overall, QDB assays are a valuable tool for rapid, cost-effective, and semiquantitative analysis of target molecules, but they have limitations in terms of dynamic range, specificity, and multiplexing capabilities when compared to other quantitative techniques. Even though they are called quantitative assays, dot blots have become increasingly deemed to be a semi-quantitative assay because their signal intensity is usually compared with an average curve based on known concentrations in target molecules. This may result in variability and errors of quantification, especially at extreme points on the standard curve.[55]

4.2 Immunochromatographic assays (ICAs)

In an immunochromatographic assay, the antigen moves upwards through the chromatography nitrocellulose paper strips dipped vertically in the vials and is detected by the antigen–antibody reaction in a similar scheme as the lateral flow assay (Fig. 2B). The ICA can detect binding by the measurement of fluorescence intensity using a laser FL scanner for corresponding analyte concentration evaluation. Since this technique could detect both free analyte and analyte bound to the serum protease, separation of serum from the whole blood can be eliminated.[56] Many fluorescently-tagged antibody labels have been developed into lateral flow assays to detect HPV biomarkers for cervical cancer diagnosis and early identification of bile duct cancer that capture IgG antibodies from human serum.[57] Detection using ICAs can be improved through precise printing of detector molecules on nitrocellulose sheets using a bio-plasmonic calligraphy system and laboratory syringe pumps.[58] Apart from antibodies, nucleic acid can also be used to detect biomarkers in a colorimetric paper assay, such as for the identification of lung cancer biomarker mir21 (microRNA). The poly(vinylidene fluoride) (PVDF) paper is impregnated with a luminescent reporter – poly(3-alkoxy-4-methylthiophene) (PT) along with the complementary strand of mir21 in the form of peptide nucleic acid (PNA). In the presence of a noncomplementary (non-target) sequence, a non-fluorescent duplex due to the electrostatic interaction between non-complementary sequences and PT gets formed. This interaction leads to fluorescence quenching and thus change of colour from orange to purple.[59] However, the presence of target DNA leads to the formation of fluorescing triplex (PT–PNA–mir21) of orange color. About 13 strains of HPV have been identified by multiplexed lateral flow assay using DNA-complementarity-based identification instead of antigen–antibody reaction.[60] Recently, a pyrrolidinyl peptide nucleic acid (acpcPNA) probe has been engineered into a fluorogenic paper-based biosensor to detect HCV cDNA, which has become a leading cause of hepatocellular carcinoma. The overhang region of the ssDNA significantly amplifies the signal, reducing the limit of detection to as low as 5 pmol.[61] Recently, the LFA platform has been extended to develop a new technique of 'SERS-LFA'(surface-enhanced Raman spectroscopy-based lateral flow assay) where the biosensor uses aptamers as the recognition element to detect thrombin and platelet-derived growth factor-BB (PDGF-BB) from prostate cancer plasma.[62] Instead of using antibody or ss-DNA, the lateral flow assay can also be modified with HPV 16 virus-like particles as probes to identify HPV antibodies from serum. Such point-of-care systems are capable of evaluating the vaccination status of a person against cervical cancer.[63]

4.3 NAAT–ICA/NAAT–LFA

The nucleic acid amplification technique has been integrated with lateral flow assays/immunochromatographic assays to form the nucleic acid amplification test—lateral flow assay (NAAT–LFA) (Fig. 2E). Immunochromatographic tests (ICTs) are being nested with PCR (polymerase chain reaction) for the identification of HPV 16 and 18 DNA. Other amplification techniques such as loop-mediated isothermal amplification (LAMP) have also been integrated with lateral flow dipsticks (LFD) to detect cervical cancer biomarkers. In yet another approach, a combination of isothermal recombinase polymerase amplification (RPA), reverse dot-blot assay (RDB), and lateral flow dipstick (LFD) has been designed to identify various genotypes of HPV viral DNA.[64–68] To reduce the time, cost, and requirement of expensive instruments to conduct PCR, interesting strategies using CRISPR–Cas systems are gaining importance. Clustered regularly interspaced palindromic repeats (CRISPR)/Cas9 is a gene-editing technology that employs 2 components: a single guide RNA to detect the target DNA sequence and a CRISPR-associated protein (Cas) endonuclease to cleave the target sequence upon homology recognition.[69] Tsou *et al.* developed a CRISPR–Cas12a system integrated with paper-based LFA for the point-of-care detection of circulating HPV nucleic acids in the plasma of cervical cancer patients. The system has an equal sensitivity with PCR at a relatively lesser cost and time (refer to Fig. 3).[70] Such systems have also been immobilized on screen-printed electrodes (like graphene oxide, In_2O_3–In_2S_3) for the label-free detection of circulating tumour DNAs.[71,72] In another approach, amplification is reached by polymerisation, where the binding of the analyte triggers a controlled free-radical polymerization which enhances the detectable signal in the paper-based device. Different cancer biomarkers such as CEA, AFP, cancer antigen 125 (CA125), and carbohydrate antigen 153 (CA153) have been identified by this method.[63,73] Advanced origami paper-based devices modified with a pyrrolidinyl PNA can be used to capture prostate cancer associate (PCA3) biomarker DNA in the clinical samples. Subsequent addition of a G-quadruplex (GQD) DNAzyme reported probe binds to the exposed sequence of PNA-bound PCA3 gene and triggers a hybridization chain reaction to accumulate more GQD onto the device. Peroxidase activity of GQD-hemin oxidizes ABTS

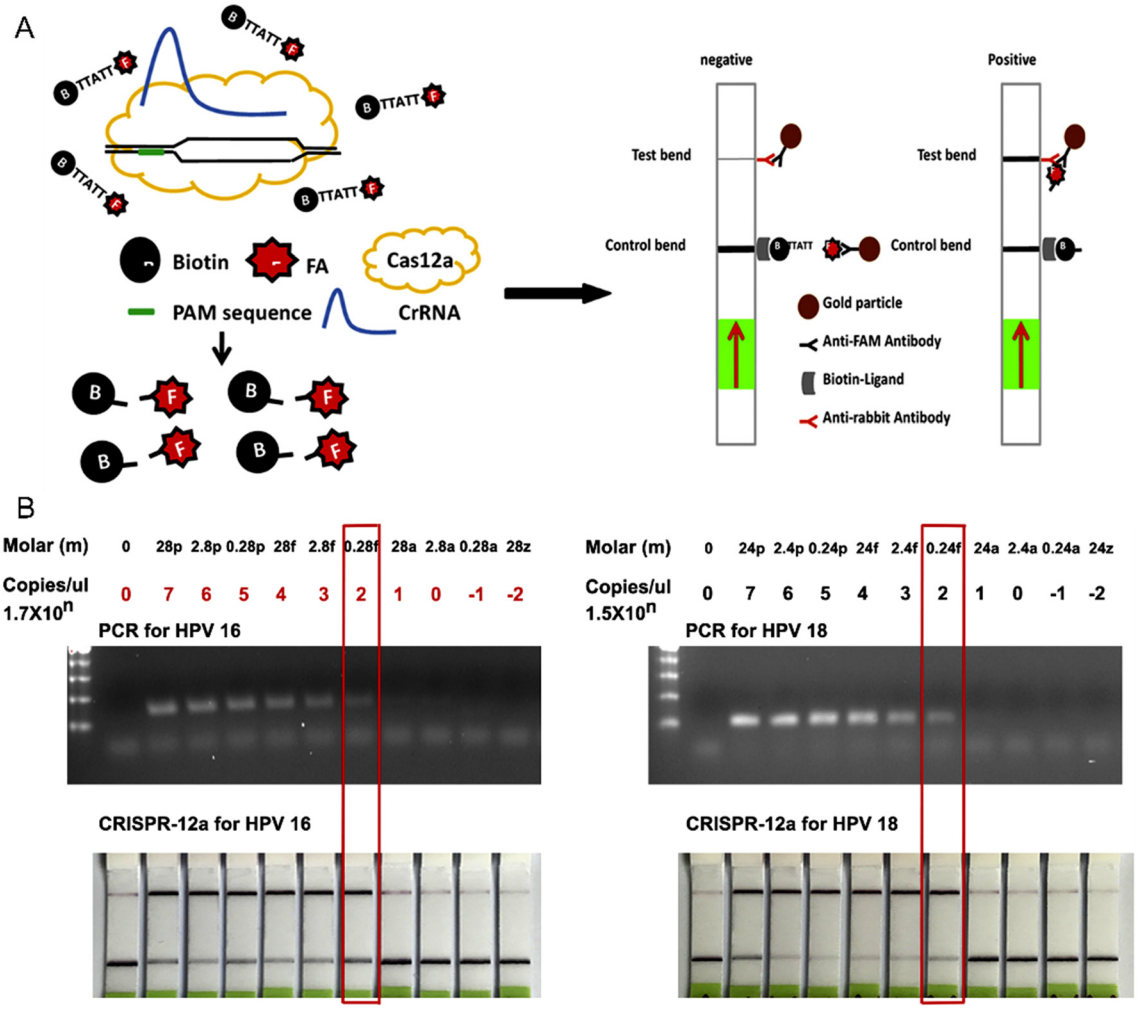

Fig. 3 Schematic of the integrated CRISPR–Cas12a system with paper-based lateral flow assay for the detection of circulating nucleic acids (A), and comparative limit of detection of HPV 16 and 18 nucleic acids by PCR and CRISPR–Cas12a system with LFA in spiked samples (B). Figures A and B have been adapted with permission from Tsou *et al.*, Translation Oncology, 2019.[70]

substrate and generates deep green color with a detection limit of 0.5 uM PCA3.[74]

4.4 Molecularly imprinted polymers (MIPs)

Molecularly imprinted polymers (MIPs) have emerged as versatile synthetic probe generation tools to recognize any epitopes on the biomarker (Fig. 2F).[75] Qi, J. *et al.* designed a movable valve microfluidic paper-based electrochemical device (Bio-MIP-ePADs), where the electropolymerization of dopamine monomers on paper substrate introduced a 'biological' molecularly imprinted polymer layer, which was used to detect CEA with a limit of detection in ng ml^{-1}. The 'artificial' synthesis of biorecognition element (dopamine in this case), eliminates the requirement of expensive and relatively unstable antibodies.[76] Fluorescent molecularly imprinting conjugated polythiophenes (FMICPs) have been used to develop MIP receptors against AFP and CEA due to their affinity for the boronate present in the synthetic receptor. This paper-based device has achieved the limit of detection in the fg ml^{-1} range, and, has been further validated with the detection of AFP in the clinical serum sample of liver cancer patients (refer to Fig. 4).[77] Imprinting of the MIP layer on screen-printed electrodes has gained attention in the last few years. The electropolymerization of phenol has enabled the synthesis of MIP receptors directly on the paper substrate to recognize 3-nitrotyrosine from urine samples.[78] The addition of poly(3,4ethylenedioxythiophene) PEDOT on the screen-printed electrodes before conjugating it with an MIP layer made of Eriochrome Black T (EBT) (as the functional monomer) can further increase the sensitivity of paper-based impedometric biosensors while detecting interleukin-β (a cancer cell proliferating biomarker whose overexpression by the inflammasomes aids in carcinogenesis).[79]

4.5 Conducting paper

Conducting paper is an ordinary paper saturated with charged nanomaterials, which increases its conductivity by

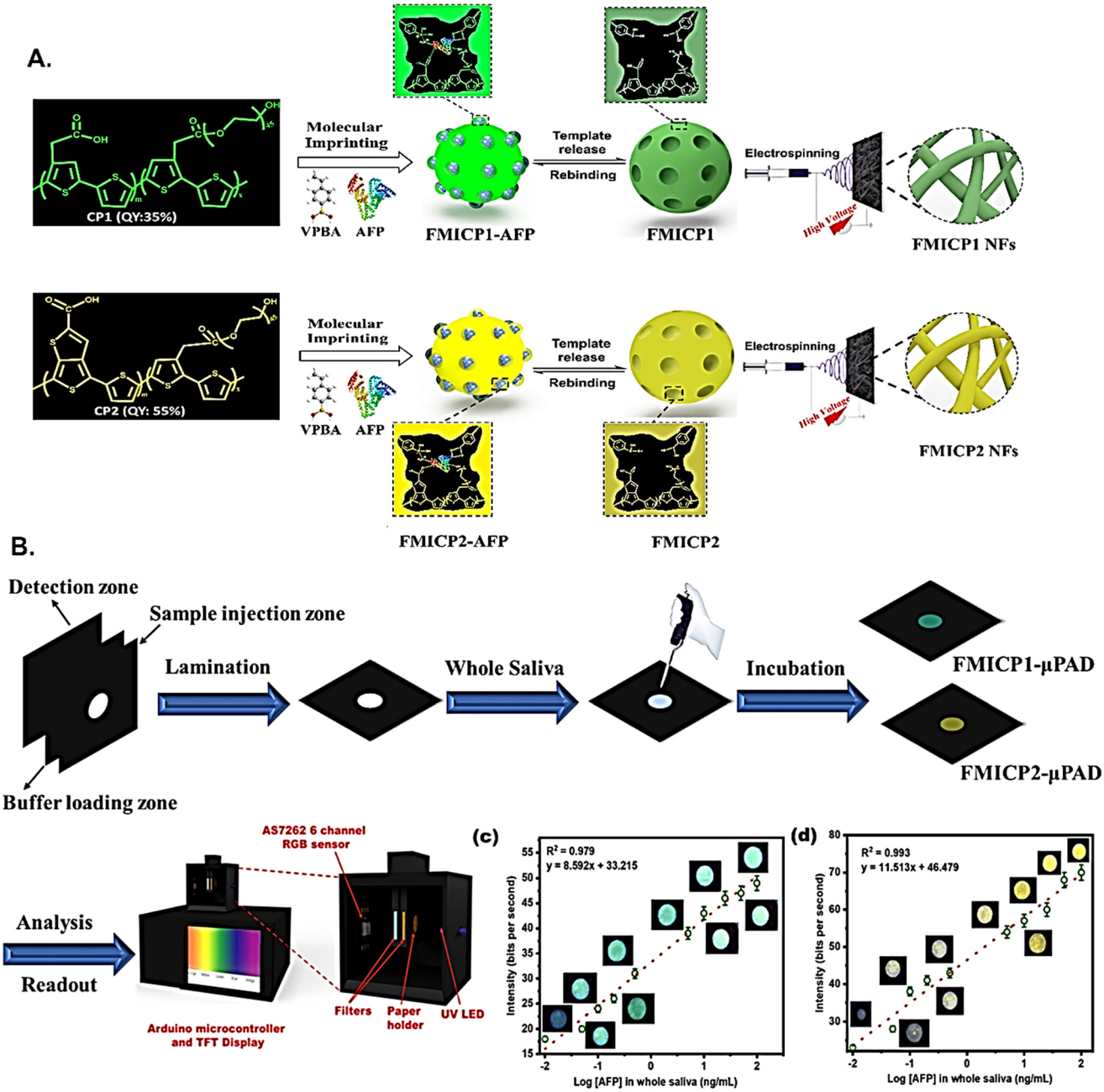

Fig. 4 A) Synthesis of molecularly imprinted nanofibres. B) Detection of AFP and CEA cancer biomarkers using MIP-coated μPAD device. Linear correlation between AFP concentration in whole saliva and the color intensity across the photodiode on C) FMICP1-μPAD and D) FMICP2-μPAD sensors. Figures A–D have been adapted with permission from Tawfik *et al.*, Biosensors and Bioelectronic, 2020.[77]

generating a potential difference across the paper as shown in Fig. 2C.[80] It requires the formation of a biological layer incorporated with nanomaterials for interaction with samples, which will be detected in the form of an electrochemical signal using a transducer. Development of paper electrodes requires a three-electrode system comprising a working electrode, a counter electrode, and a reference electrode. All these electrodes are deposited within the paper using conducting inks *e.g.*, carbon inks, silver inks, or gold inks, which enhance the conductivity of the device. For manufacturing paper-based electrodes using plastics, ceramics, and other resources as matrix materials, screen printing fabrication is used.[81]

The development of 'conducting paper' has led to many advancements in cancer detection. Paper electrodes are used for the detection of CEA up to 10 pg ml^{-1} upon immobilization of graphene/gold nanoparticles nanocomposites with high sensitivity, specificity, and stability.[82] Such conducting paper strips can be developed by immersing nitrocellulose strips into poly(3,4ethylenedioxythiophene):poly(4-styrene sulfonate) (PEDOT:PSS) polymer followed by immobilization of CEA protein or CEA-aptamers. Any binding event on this conducting

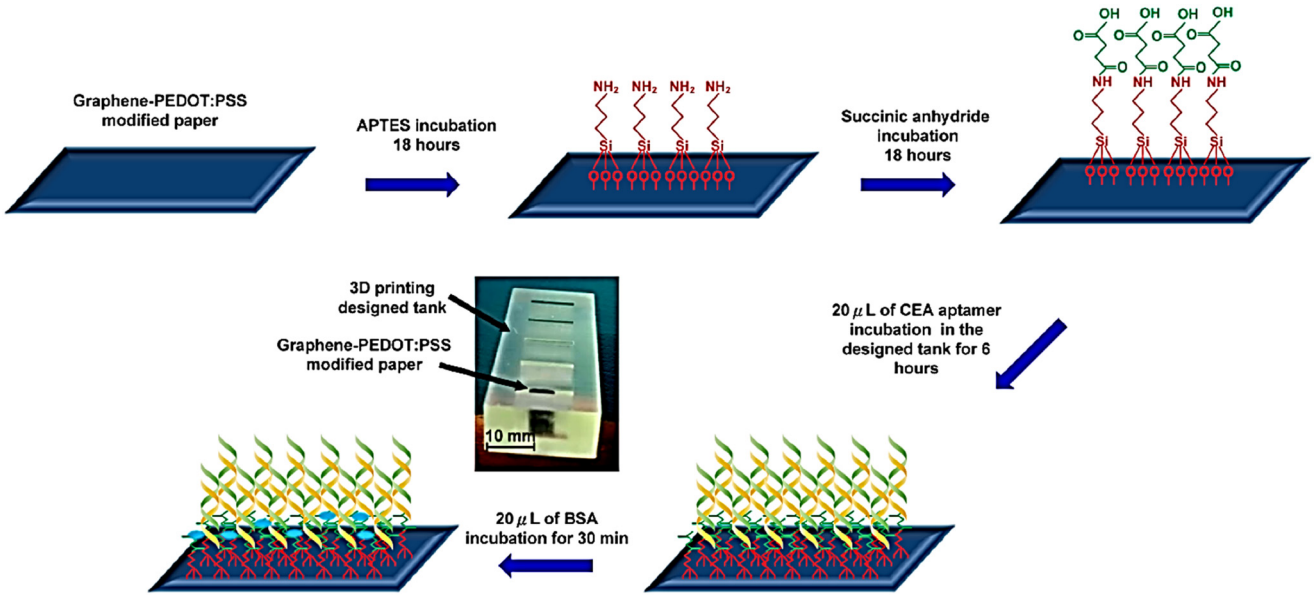

Fig. 5 Surface functionalization of conductive paper-based biosensor. Figure has been adapted with permission from Yen *et al.*, Sensors, 2020.[84]

polymer layer translates to an electrochemically measurable signal with a high sensitivity of detection (refer to Fig. 5).[83,84] Graphene ink or reduced graphene oxide is generally added to the polymer layer to increase the conductivity of paper.[84,85] Detection of analyte can also be achieved using phthalocyanine-BODIPY dye to detect CYFRA 21 (a lung cancer biomarker), as it can develop a porous structure on the conducting substrate to allow a change in conductance during analyte passage.[86] Recently, the ePADS (electrochemical paper-based analytical device) which uses screen-printed graphene electrodes has been automatized by incorporating dual-flow behaviors in a single paper-based platform. This eliminated the need for multi-step reagent manipulation and has been demonstrated to successfully detect HCV antigen at an LOD of 1.19 pg ml^{-1} from the serum of patient.[87]

5. Advancements in signal enhancement with next generation nanomaterials

Integration of a wide variety of nanomaterials to the paper-based LFAs and microfluidic devices is gaining significant importance as they can enhance the biosensor's performance by providing highly active surface, rich chemistry for easy functionalization with multiple biorecognition molecules, inherent optical properties, high electrical conductivity, and surface plasmon-related electromagnetic fields for fluorescence quenching, and color changes.[88,89] These nanomaterials have been systematically classified into inorganic, organic, and hybrid and their role in amplifying the colorimetric, fluorescence, and electrochemical-based signal for cancer biomarker detection with enhanced sensitivity and limit of detection has been well explained in this section (refer to Fig. 6).

5.1 Inorganic nanomaterial-based biosensors

Inorganic nanomaterials comprise quantum dots, metallic nanoparticles (gold, silver), magnetic nanoparticles, and upconversion nanoparticles. These nanoparticles are attractive for their size and shape-dependent tunable physical (optical, magnetic properties) and chemical properties (stability, inertness).[90]

5.1.1 Metallic nanoparticles. These nanoparticles are composed of metals such as gold, silver, platinum, *etc.* with size and composition dependent optical and electronic properties.[91] Gold nanoparticles (AuNPs) are the most commonly used metallic nanoparticles in biosensors and are also predominantly used to develop lateral flow paper-based colorimetric assays. Biocompatibility of AuNPs and its surface functionalization with proteins through covalent bonds between gold atoms and protein's amine and cysteine groups help stabilize the sensing proteins and their biological activity.[91] Depending on the application, AuNPs can be used in various forms such as gold nanoclusters (AuNCs), gold nanorods (AuNRs), gold nanostars (AuNSs), and gold nanoseeds.[92]

Abarghoei *et al.* reported a AuNCs-based Y-shaped microfluidic biosensor for the detection of prostate cancer using citrate as an early biomarker. AuNCs capped with cysteine (Cys–AuNC) possess peroxidase activity that can oxidize 3,3′,5,5′-tetramethylbenzidine (TMB) in the presence of H_2O_2 to blue color in the absence of citrate. However, in prostate cancer patient samples, the citrate biomarker inhibits the peroxidase activity of Cys–AuNCs and prevents the color change by blocking TMB oxidation.[93] A similar

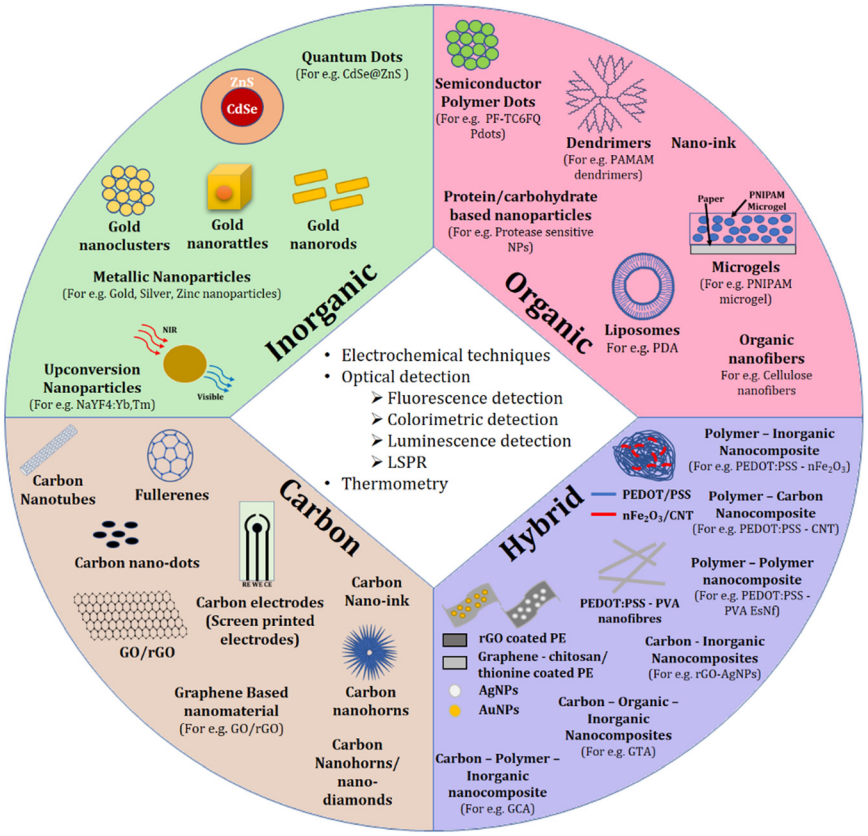

Fig. 6 Types of particles used for paper-based biosensors. μPADs – microfluidic paper-based analytical devices, AgNPs – silver nanoparticles, CdSe@ZnS – cadmium selenide–zinc sulfide, CNT – carbon nanotube, EsNf – electrospun nanofibers, GCA – graphene–chitosan with gold nanoparticles (AuNPs), GO – graphene oxide, GTA – graphene/thionine/AuNPs, LSPR – localized surface plasmon resonance, nFe_2O_3 – nanostructured iron oxide, PAMAM – polyamidoamine, PDA – polydiacetylene, Pdots – polymer dots, PE – paper electrode, PEDOT:PSS – poly(3,4-ethylenedioxythiophene):poly(4-styrenesulfonate), PNIPAM – poly(*N*-isopropylacrylamide), PVA – polyvinyl alcohol, rGO – reduced graphene oxide.

approach has also been used for colorimetric aptasensing of CEA over a range of 4 to 25 ng ml^{-1} with 100% sensitivity and around 97% specificity. The aptasensor employs mercury ions (Hg^{2+}) to block the TMB-reducing capability of AuNPs during CEA detection by the aptamer and in turn imparts a reduction in the blue color.[94] AuNRs are also used for cancer detection due to their high surface area, improved signal-to-noise ratio, and high electrical conductivity leading to better electron transfer as compared to AuNPs.[95] Electrochemical techniques such as cyclic voltammetry (CV), differential pulse voltammetry (DPV), electrochemical impedance spectroscopy (EIS), amperometry, which sense the analyte based on current change with respect to voltage, change in impedance over a range of frequencies (EIS), change in current with respect to time (amperometry) due to antigen–antibody interactions can also involve the use of AuNRs as biosensing element.[96] CV measures current upon linearizing the potential of a working electrode with time. The potential is generally measured on a cyclical basis from two limits that are normally forward and backward.[97] On the contrary, DPV involves the use of several possible pulses to an active electrode with low amplitude and short duration coupled onto a linear sweep of impulses.[97] In comparison with traditional voltammetry techniques, the resulting current shall be recorded differentially to provide enhanced sensitivity and resolution. CV and DPV, with their distinct advantages and applications, are the most widely used electroanalytical techniques.[97] While CV provides information on redox behavior and kinetics for electrochemical reactions in a range of potentials, DPV offers enhanced sensitivity and selectivity, which makes it particularly suited to trace analysis and the quantification of analytes. EIS is also a very powerful technique to analyze the electrical response of an electrochemical system, with regard to applied alternating current signal at various frequencies.[98] It provides information on the electrochemical processes occurring on the surface of the electrode and on the properties of the electrolyte solution. Amperometry is used in response to chemical species undergoing oxidation or reduction on an electrode and measures the current at a specific potential. It is frequently used for the detection and quantification of analytes with high sensitivity.[99] A special form of gold nanomaterial called gold nanorattles (AuNRTs), which are hollow plasmonic nanostructures, have also been used for the diagnosis of renal cancer by detecting perilipin-2 (PLIN-2) biomarkers. They consist of an AuNP core with a porous and cubic Au shell and exhibit higher refractive index

sensitivity as compared to solid nanostructures (such as AuNRs) for localized surface plasmon resonance (LSPR).[100]

Similar to gold nanoparticles, silver nanoparticles can also be employed in paper-based electrochemical sensors owing to their high biocompatibility and electrical conductivity.[91] Nanoporous silver, AuNRs, and AuNP inks can be coated onto cellulose fibres to generate paper working electrodes, that can be immobilized with cancer biomarker-specific primary antibodies for electrochemical detection of antigens like PSA, CEA, and AFP. Metallic nanoparticles and nanocomposites like porous zinc oxide spheres–silver nanoparticles (PZS–AgNPs) composite are also used to amplify biosensing signal upon immobilization with secondary antibody (refer to Fig. 7).[101–103]

Even though, gold and silver nanoparticles are predominant choices for electrochemical biosensors, numerous other metals like platinum, copper, nickel, palladium, and iridium also possess significant catalytic properties that can help design low-detection and high-sensitivity sensors. Even though their application has not been explored much in paper-based biosensing, they possess great potential in the detection of oligonucleotides, carbohydrate, and peptide moiety, and as electron transfer intermediates in electrochemical sensors.[91,104]

5.1.2 Quantum dots. Another type of inorganic nanocrystal are the quantum dots (QDs) which are made up of semiconductors like cadmium telluride (CdTe), zinc selenide (ZnSe), *etc.* with unique properties such as broad absorption with narrow fluorescence emission, size/structure/composition tunable emission from visible to IR region, and exceptional brightness due to high quantum yields.[105] QD nanoparticles consist of a large number of metal ions which results in enhanced voltammetric signals when used as a label as compared with metal ion label.[106] QDs can overcome the limitations associated with immunochromatographic electrochemical biosensors (IEB) like low voltammetric signals because of lesser metal ions present per antibody molecule and the inability to detect low concentrations of biomarkers. Hence, IEB consisting of CdSe@ZnS QDs conjugated with anti-PSA antibodies (anti-PSA-QDs) are used for the detection of prostate cancer-specific PSA biomarker in an LFA. The LFA-based detection of PSA antigen is quantified using a screen-printed electrode present inside the test zone employing square wave voltammetry (SWV).[107] CdTe QDs immobilized onto the paper can also be used for CEA detection in a silver ion-dependent manner. Acidic treatment of anti-CEA antibody labeled AgNP post CEA capturing can lead to the dissolved Ag ions induced fluorescence quenching of CdTe QDs as a concentration-dependent readout with a detection limit of 5.6 pg ml^{-1}.[108] CdTe/CdSe QDs impregnated paper can also be coupled with enzymes like glucose oxidase for the H_2O_2-based fluorescence

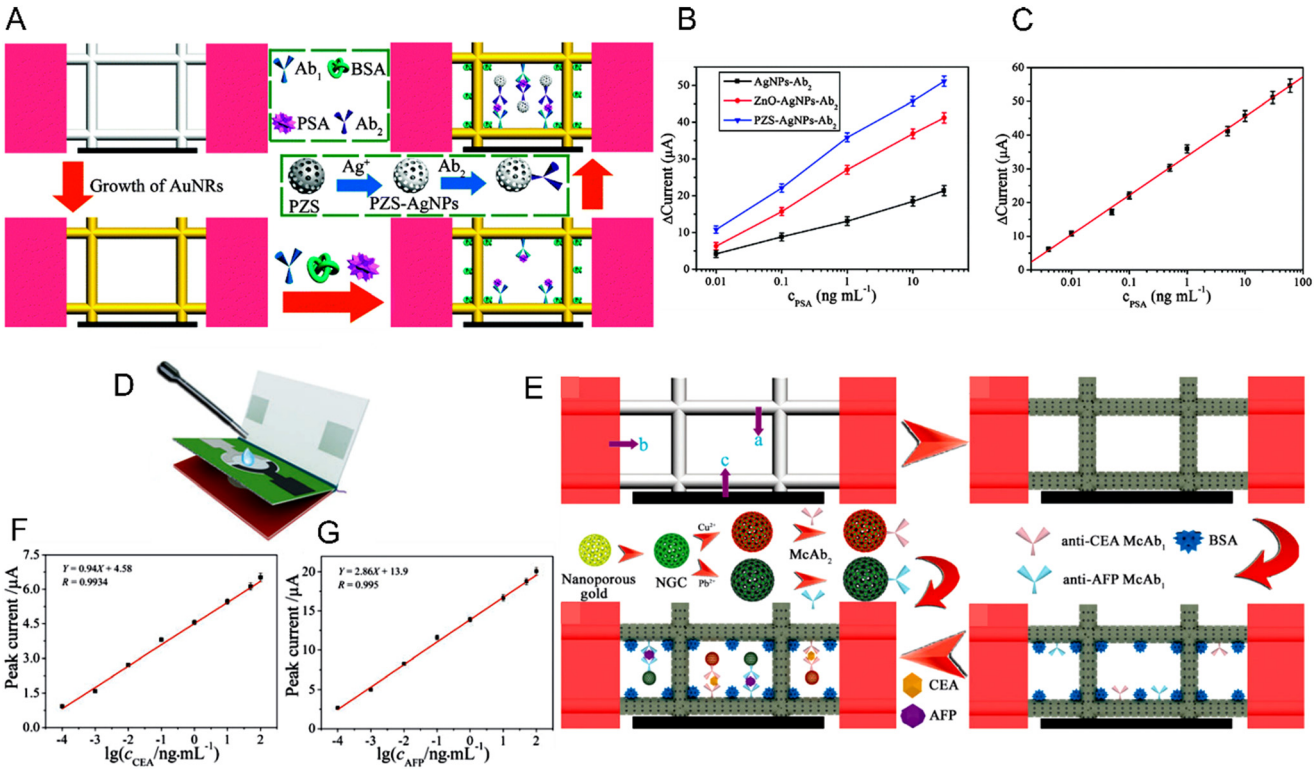

Fig. 7 Schematic of the gold nanorods coated paper-based electrochemical immunosensor containing porous zinc oxide spheres–silver nanoparticles nanocomposites as detection labels (A), the effect of different detection labels on prostate-specific antigen (PSA) concentration-dependent current generation (B), and a calibration curve of PSA using electrochemical immunosensor (C). Schematic of 3-D origami multiplexed electrochemical immunodevice (D), steps involved in its generation using nanoporous silver coating as an electrode, and chitosan-coated nanoporous gold as detection labels for CEA and AFP (E), a calibration curve of CEA (F), and AFP (G). Figures A–C have been adapted with permission from Sun *et al.*, New Journal of Chemistry, 2015.[101] Figures D–G have been adapted from Li *et al.*, Chemical Communications, 2013.[102]

quenching readout in the presence of an analyte.[109] QDs can also be used with other metallic nanoparticles and metal–organic frameworks for the detection of the gaseous biomarkers in lung cancer patients.[110]

5.1.3 Upconversion nanoparticles. A different category of inorganic NPs namely, upconversion nanoparticles (UCNPs) is typically composed of inorganic host matrix doped with metals such as lanthanides.[111] These nanoparticles possess the ability to emit visible luminescence under NIR excitation and are preferred over conventional fluorophores due to their unique properties of sharp emission band and high photostability.[112] UCNPs employ fluorescence resonance energy transfer (FRET) and can be used for the multiplex detection of cancer biomarkers like CEA, α-fetoprotein (AFP), and carbohydrate antigen-125 (CA-125). In such biosensors, anti-CEA linked polyethyleneimine (PEI) modified $NaYF_4$:Yb,Tm UCNPs are printed on the normal filter paper as FRET donors and CEA labeled fluorescein isothiocyanate (FITC) as FRET acceptor. Interaction of biomarker and antibody results in an energy transfer from Tm^{3+} to FITC and subsequent fluorescence emission at characteristic wavelength is monitored for cancer detection.[113] A smartphone-coupled lateral flow strip sensor was also reported for the detection of PSA and EphA2 cancer biomarkers using anti-PSA antibody tagged Er3+-doped UCNPs as well as anti-EphA2 antibody-tagged Tm3+-doped UCNPs. The binding of PSA and EphA2 antigens to their respective antibodies tagged UCNPs present on the device emits yellow and purple upconversion signals which indicates the presence of PSA and EphA2 respectively.[114]

5.1.4 Carbon based nanomaterials. The unique combination of superior optical, electrical, and mechanical properties makes carbon allotropes a favored nanomaterial in the biosensing of cancer-specific markers.[115] Based on their unique properties carbon-based nanomaterials have been used as graphene sheets, graphene quantum dots, carbon nanotubes (CNTs), carbon quantum dots/carbon nano-dots (C-dots), fullerenes, carbon nanohorns, or carbon nanodiamonds.

Graphene is a 2-dimensional flat sheet of hexagonally arranged carbon lattice. Graphene-based biosensors gained popularity in biosensing applications in the form of graphene-oxide sheets, graphene paper-electrodes, and graphene quantum

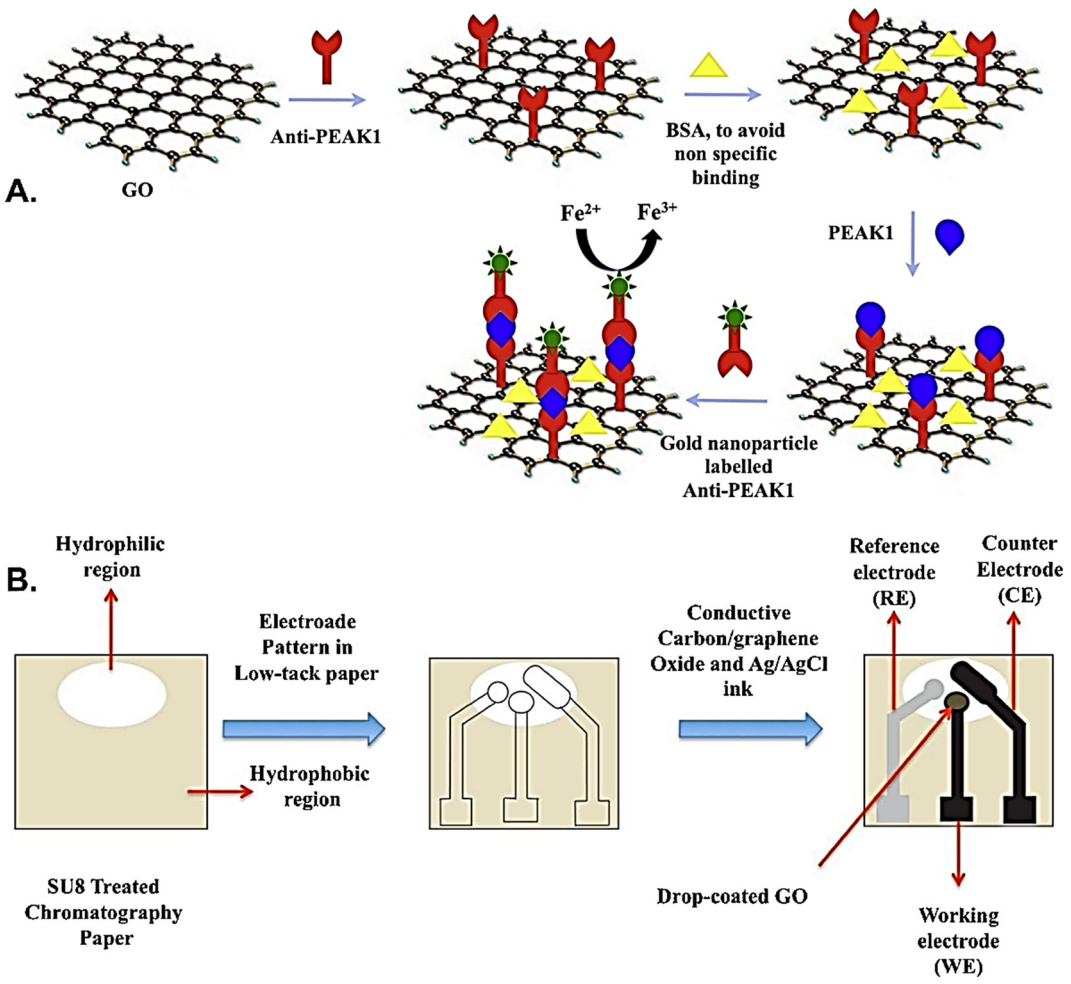

Fig. 8 A and B) Paper coated graphene oxide based immunosensor for pancreatic cancer biomarker (PEAK1 tyrosine kinase) detection. Figures A and B have been adapted from Prasad *et al.*, Sensors and Actuators B: Chemical, 2020.[119]

dots.[116] Graphene-oxide modified microfluidic analytical devices were developed for the detection of cancer cells (MCF-7, HL-60, and K562 cells). DNA-aptamer functionalized coloured quantum dots are adsorbed on the graphene paper nanosensor, where a fluorescence signal is detected based on FRET upon biomarker analyte binding.[117] Graphene-oxide or reduced graphene oxide nanocomposites have also been used to modify the paper electrodes for electrochemical sensing of PSA, CEA, pancreatic cancer biomarker $PEAK_1$, and cancer antigen 125 (refer to Fig. 8).[118–121] Graphene-based nanomaterials can also be used for the development of dot immune-graphene–gold filtration assay (DIGGFA) exploiting the photothermal effect of graphene oxide nanocomposites to detect MCF-7 breast cancer cells, portable 3D-μPAD functionalized with graphene nanocomposites to detect α-fetoprotein, and graphene oxide screen printed electrodes (GPHOXE) to detect circulating tumour DNAs.[71,122,123] Apart from the graphene-oxide sheets and graphene paper electrodes, graphene quantum dots are emerging as new 'nano-biosensor' probes for cancer detection.[124] Graphene quantum dots with multi-walled carbon nanotubes (MW-CNTs) can significantly amplify the sensitivity of detection to up to 0.03 ng ml^{-1} for the simultaneous quantification of 2 metastatic biomarkers (IL-13Rα2 and CDH-17) from breast and colorectal cancer cell lysate samples and paraffin-embedded tumour tissues within 3 hours.[125]

CNTs on the other hand are rolled-up large cylindrical hollow tubes of single (single-walled CNTs) or multiple sheets of graphene (multi-walled CNTs).[126] Their distinctive features such as special geometrical shape, high conductivity and chemical stability, high aspect ratio, and lightweight with good mechanical strength makes it a suitable candidate for biosensing platform.[127] Carbon nanotubes can offer electrical conductivity 100 times higher than copper along with mechanical strength better than that of steel and even superior thermal conductivity than diamond.[128] Exemplary properties of CNTs can be imparted onto the paper-based sensors by loading antibody-modified multi-walled CNTs onto micro-porous papers. Any binding event on the surface of the antibody results in a shift of electron transfer in the sensor, leading to a change in resistance that can be recorded in impedimetric sensors.[129] These conducting paper electrodes can be a great low-cost yet sensitive alternative to the advanced ionic liquid CNT-modified electrodes, advanced quantum dots attached CNTs based electrochemical sensors, or CNT field-effect transistor based biosensors.[129–131] Even a primary antibody-attached multi-wall CNTs modified paper biosensor could impart a noteworthy detection limit of 1.18 ng ml^{-1} for PSA as compared to commercially available ELISA kits (51 pg ml^{-1}).[129] Application of CNTs has also been extended to the detection of human fetuin A (HFA) (a pancreatic and liver cancer biomarker) and miR-141 (prostate cancer biomarker) by functionalizing onto screen printed carbon electrodes (SPEs) and electroactive polymer printed electrodes respectively.[132–134] These discovered 'nano-probes' of carbon allotropes integrated with paper-substrate can help in achieving a quantifiable and highly sensitive electrochemical/amperometric/fluorometric nano-biosensor with a strong potential for translation in clinical settings. In conclusion, superior conductivity, ease of functionalization, and tunable signal enhancement properties make inorganic nanomaterials extremely important for the development of advanced paper-based biosensors for cancer detection.

5.2 Organic nanomaterial based biosensors

In addition to inorganic nanomaterials, different kinds of organic nanoparticles (polymer dots, liposomes, dendrimers, nanofibres) have also been employed for the paper-based detection of cancer biomarkers by exploiting the unique properties of biomolecules.

5.2.1 Semiconductor polymer dots. Fluorescence-emitting semiconductor polymer dots (PDOTs) are superior fluorescent lateral flow assay probes due to their easy surface functionalization and significantly higher brightness per unit probe. PDOTs can detect multiple cancer biomarkers on a single immunochromatographic test strip (ICTS). Even though, inorganic quantum dots having exceptional photophysical properties could be a better choice in ICTS, their active interaction with biothiols/metal ions in body fluids and damaging toxicity to the environment limits its applications.[135–138] PDOTs on the other hand not only offer superior fluorescence brightness than quantum nanocrystals, but also offer a high signal-to-noise ratio, high colloidal and photostability in biological fluids, and amplified energy transfer with multicolor emissions for multiplexed detection of biomarkers under single excitation wavelengths.[139–141] Researchers have developed versatile platforms for cancer detection by incorporating semiconducting polymers into nanoparticles, utilizing PCA (poly(9,9-dioctylfluorene)-co-phenylene) as one such approach. The fluorescent signal emitted by PCA nanoparticles can be amplified through various methods, such as Förster resonance energy transfer (FRET) or aggregation-induced emission (AIE), enhancing the sensitivity of cancer detection assays. FRET between antigen-capturing PCA nanoparticles and antigen-detecting PF-TC6FQ Pdots in an ICTS due to their overlapping emission and absorption spectra respectively, can give a visual hue of emission from sky blue to orange-red under 410 light exposure which can be correlated with the antigen concentration in the samples (refer to Fig. 9).[142] PDOTs may also be used to multiplex the detection of cancer biomarkers such as AFP, CEA, and PSA using semi-conducting polymers with distinct emission colors [PF-TC6FQ (red), PFO (blue), and PFCN (green)].[142,143] PDOTs can also be modified to have a broad excitation range and emit ultrabright NIR with large stokes shifts by using quinoxaline derivatives and their varying molar percentages in the polymer backbone. Such quinoxaline based PDOTs were observed to be 8 times more brighter than commercial quantum dots (Qdots655).[144] Quinoxaline-based dual colorimetric and fluorometric paper strips have been developed to detect the acidic pH of biofluids associated with tumor growth.[145] The PDOT-based

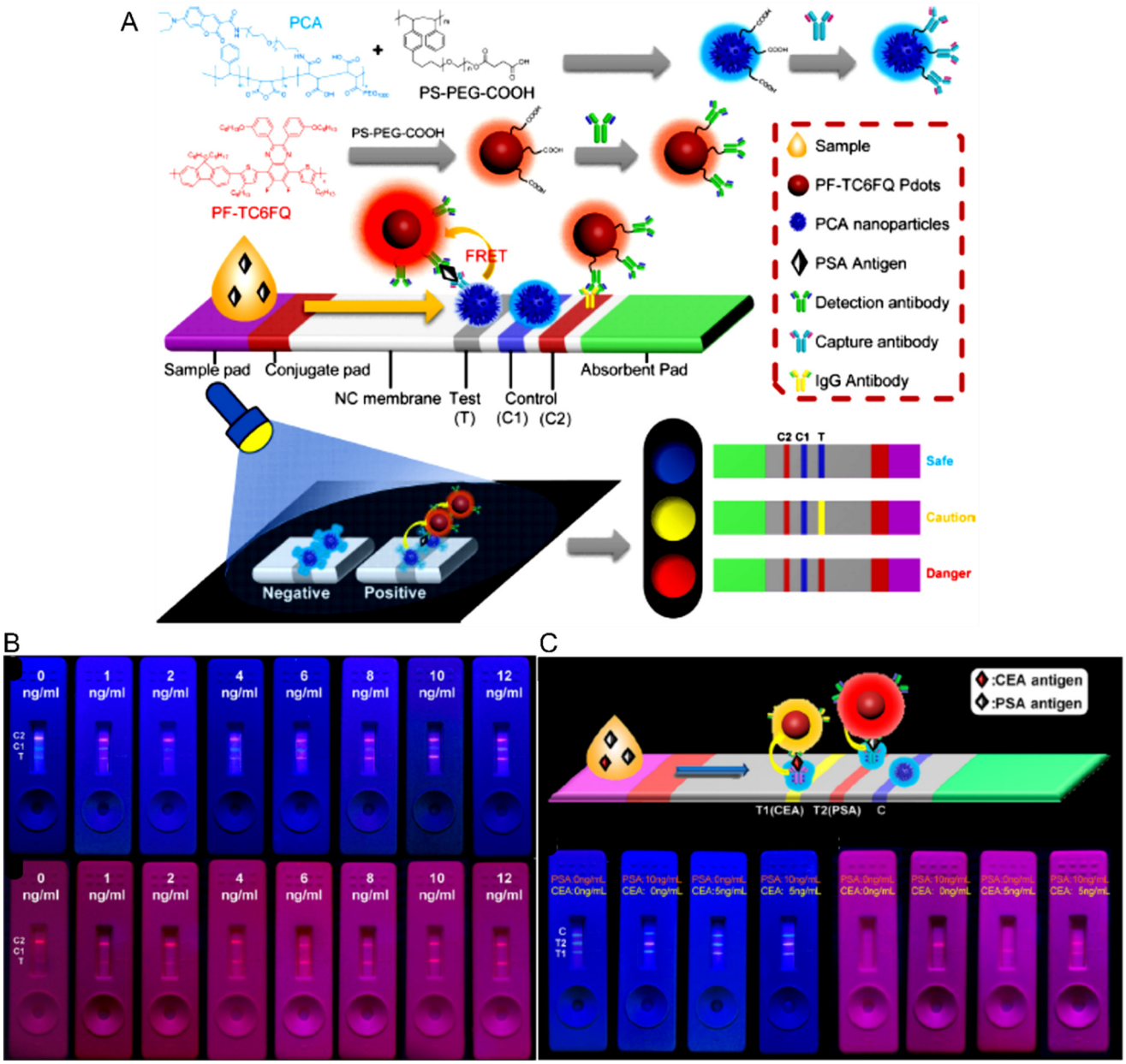

Fig. 9 Schematic of FRET-created traffic light immunochromatographic strip (ICTS) for the cancer biomarker detection (A), photographic images of ICTS detecting different concentration of prostate specific antigen (PSA) biomarker upon excitation under 410 nm UV light (blue panel) and its corresponding fluorescence with a 600 nm long-pass filter (purple panel) (B), and multiplex detection of dual biomarkers (CEA and PSA) using FRET-created ICTS (C). Figures A–C have been adapted with permission from Yang *et al.*, Analytical Chemistry, 2020.[142]

probes have also emerged as colorimetric readouts in immunochromatographic tests for PSA biomarker identification with ~pg ml^{-1} limit-of-detection.[146]

5.2.2 Liposomes. These are small polymeric vesicles of spherical shape that can be formed using natural phospholipids surrounding an aqueous core.[147] Liposomes are predominantly used to enhance the limit of detection of colorimetric low-cost paper-based sensors for early diagnosis. They are generally employed in polymerization-based signal amplification (PBA) chemistry, where they can be encapsulated with large amount of photoinitiators like eosin Y to overcome limited photo-initiation reaction due to poor solubility and fluorescence self-quenching of photoinitiators.[148] High photoinitiator encapsulation and their rapid localized release from liposomes in the presence of target analyte can enhance free-radical polymerization on biofunctionalized paper to generate colored hydrogels.[148] Liposomes can easily load different types of hydrophilic and hydrophobic dye molecules with high loading capacity and can impart an application-specific sustained or rapid triggered release profile.[149] Incorporation of liposomes into PBA could enhance the signal by 30-fold compared to conventional PBA and increase the detection limit to sub-nanomolar range with high contrast signals.[148] High biocompatibility of lipid-based nanocarriers also reduces non-

specific interactions with biological fluid components and thus can be employed as signal enhancers in low-cost biosensing applications.[150] Liposomal building blocks *i.e.* phospholipids (distearoyl phosphatidyl ethanolamine–polyethylene glycol, DSPE–PEG), monoacyl C18 fatty acids, or cholesterol are also used to detect exosomes present in the blood of cancer patients.[151] Exosomes are small (30–100 nm) membrane-bound vesicles secreted by the mammalian cell including cancer cells and can be a great prognostic marker for cancer detection. These amphiphilic probes can be inserted into exosomal membrane *via* their hydrophobic tail and can be tagged with biotin on the hydrophilic end for efficient exosome isolation from the clinical samples.[152]

5.2.3 Dendrimers. These are nano-sized symmetrical molecules with a well-defined shape and homogenous distribution of systematic branching around them and are mostly characterized as highly functional nanomaterial due to the presence of functional groups.[153,154] A 5th generation polyamidoamine PAMAM dendrimer with 128 amino functional groups on its outer surface was immobilized onto the paper surface for the detection of telomerase enzyme.[155] This enzyme is reactivated in almost 85% of the cancer cells and can promote indefinite cell proliferation by preventing telomeric shortening due to its DNA polymerase activity.[156] Telomerase substrate (TS) primer molecules were then attached to the dendrimer surface which will be subsequently amplified by the telomerase present in the clinical sample. The telomerase extension products can be detected by Cy5 labeled ss-DNA probes for a fluorescent readout. Multiple functionalizing sites on a branched dendrimer provide an advantage to developing an amplification-free, fast, low-cost, and instrument-free assay.[155]

5.2.4 Organic nanofibers. The porosity of the paper is an important governing factor of paper-based test strip sensitivity.[157] Reducing the pore size can significantly enhance the sensitivity however its adjoining side effects like reduced sample flow, increased assay time, complete flow stop, or membrane defects can lead to compromised reproducibility.[158] Therefore, organic nanofibers like cellulose nanofibers (CNFs) can be specifically used to increase the pore size of the test region where detection antibodies are embedded.[159,160] Biocompatibility and gel-based easy application of such nanomaterials at the localized test region can provide high surface area and superficial attachment of the recognition antibodies or the transducer particles like AuNP on the paper strip for around 36.6% enhanced colorimetric sensitivity over conventional LFAs.[161] Organic nanofibers made of PEDOT:PSS polymer can also be used to develop conducting paper electrodes for electrochemical sensors.[162] These polymers can be electrospun onto the paper as long ultrafine fibres to impart electrochemical properties, thermal stability, mechanical strength, and high surface-to-volume ratio for enhanced biomolecule loading, and efficient biochemical interactions.[162,163] Biofunctionalization of these nanofibers with CEA antibodies can detect CEA in a linear range of 0.2–25 ng ml^{-1} with high sensitivity.[162] This can provide a great alternative to the costly metallic printed electrodes having silver, gold, or graphite inks and develop cost-effective, flexible, biocompatible, and disposable paper-based sensors.[162]

5.3 Multi-nanomaterial based hybrid biosensors

Each nanomaterial possesses unique properties that can be utilized to enhance antigen capture, detection, and signal amplification, however in order to enhance the overall sensitivity, specificity, and efficiency of a biosensor, a rational amalgamation of multiple nanomaterials or combination of nanomaterial with special polymers would be ideal. For example, in addition to the use of conducting polymers like PEDOT:PSS for the fabrication of conducting paper, the use of PVA-nanofibres, nanostructured iron oxide, reduced graphene oxide (rGO), and CNTs can increase the sensitivity, specificity, and robustness of a biosensor by improving its mechanical strength, electrochemical activity, and cancer biosensing properties.[85,162,164,165] Similarly, a novel ink-jet printed photo paper-based biosensor can be coated with conductive silver nanoparticles (AgNPs) and rGO-based nano ink (Ag/rGO), where Ag/rGO nano-ink was used synergistically with cysteamine doped AuNPs (CysA/AuNPs) as signal amplification labels for the chronoamperometric detection of breast cancer-specific carbohydrate (CA 15-3). This increased the electron transfer efficacy and biosensor efficiency due to the synergistic use of signal amplification labels as well as hybrid nanocomposite of carbon-based (rGO) and inorganic nanomaterials (AgNPs).[166–168] GQDs with Au–Pd alloy nanoparticle (NPs) probes can be used to quantify H_2O_2 released by tumor cells by both photoelectrochemical as well as colorimetric transduction, whereas when used with reduced-graphene quantum dots and chitosan, they can fluorescently detect alkaline phosphatase (ALP)—a bone, breast, and ovarian cancer biomarker.[169,170]

Another interesting hybrid strategy involved the use of graphene–polyaniline modified paper electrodes (G-PANI) for the electrochemical detection of HPV nucleic acid. Anthraquinone-labeled peptide nucleic acid (ss-PNA) probe was functionalized on the G-PANI surface for capturing complementary target DNA of HPV. Upon sample addition, the PNA-target DNA construct blocks the charge transfer from anthraquinone to G-PANI conducting paper surface and reduces the current. This reduction in the current signal correlates with the presence of HPV DNA for cervical cancer diagnosis.[171] Xia *et al.* have also reported a paper-based thin film microextraction system that can detect gaseous benzaldehyde (BA) in human exhalation as a biomarker for Lung Cancer using metal–organic framework (MOF such as NU-901) structures embedded with gold nanorods and quantum dots (GNRs-QDs@NU-901) in dual mode *i.e.* fluorescence detection as well as SERS signal quantification.[110] Therefore, when BA encounters these structures, its aldehyde group interacts with the amine group of 4-mercaptonoaniline present on GNRs and this results in

the formation of Schiff base, which in turn, causes disassembly of GNRs and QDs, resulting in fluorescence signal. On the other hand, the formed Schiff base was also used as a SERS reporter for BA detection.[110]

A hybrid rGO-modified paper electrode coated with branched zinc nanorods (BZR) instead of AuNRs alone can also be used for enhanced immunosensing of α-fetoprotein (a tumor biomarker) due to increased sites for antibody loading, along with the synergistic use of porous zinc oxide spheres–AuNPs (PZS@Au) nanocomposites as signal labels.[103,172] A similar strategy including SiO_2 nanoparticles, chitosan, and graphene was also integrated into a paper-based microfluidic device for the multiplex detection of four kinds of cancer biomarkers such as CEA, AFP, CA125, and CA153. To remove the complexity due to the presence of labels, a novel label-free microfluidic-based electrochemical (EC) immunosensor was developed for the detection of CEA by coating the working paper electrode with antibody-linked carbon-organic–inorganic (graphene–thionine–AuNPs) hybrid nanocomposites. Thionine being an electrically active substance was employed for current generation due to redox reactions, whereas amino-functionalized graphene was used for signal amplification by accelerating the electron transfer due to its excellent conductivity.[82] Further advancements in the same immunosensor have been made for the simultaneous detection of dual cancer biomarkers (CEA and lung cancer-specific neuron-specific enolase (NSE)). Working electrodes were modified with graphene–thionine–AuNPs nanocomposites and Prussian blue (PB)–poly (3,4-ethylenedioxythiophene) (PEDOT)–AuNPs nanocomposites to immobilize CEA aptamer and NSE aptamers respectively and enhance electron transfer. An improved limit of detection of 2 pg ml^{-1} for CEA and 10 pg ml^{-1} for NSE was observed along with correlating efficacy with commercially available equipment for detecting biomarkers in clinical serum samples (refer to Fig. 10).[116] Since EC sensors are less portable and relatively costly due to the requirement of heavy and costly instrumentations, a novel battery-triggered electrochemiluminescence (ECL-luminescence generated during electrochemical reaction) based immunosensor using dual-signal amplification strategy was developed for the detection of PSA and CEA. It is a microfluidic device with wax-patterned paper (with screen-printed electrodes) employing a hybrid of graphene oxide–chitosan–gold nanoparticle as an immunosensing platform and functionalized nanoporous silver as signal amplification labels.[173]

Immunoassay-based multi-readout biosensing of cancer biomarkers like PSA can also be achieved through a photothermal biosensing lab-on-a-chip. A PMMA paper hybrid disk consisting of a dissociative clip unit and a magazine bearer

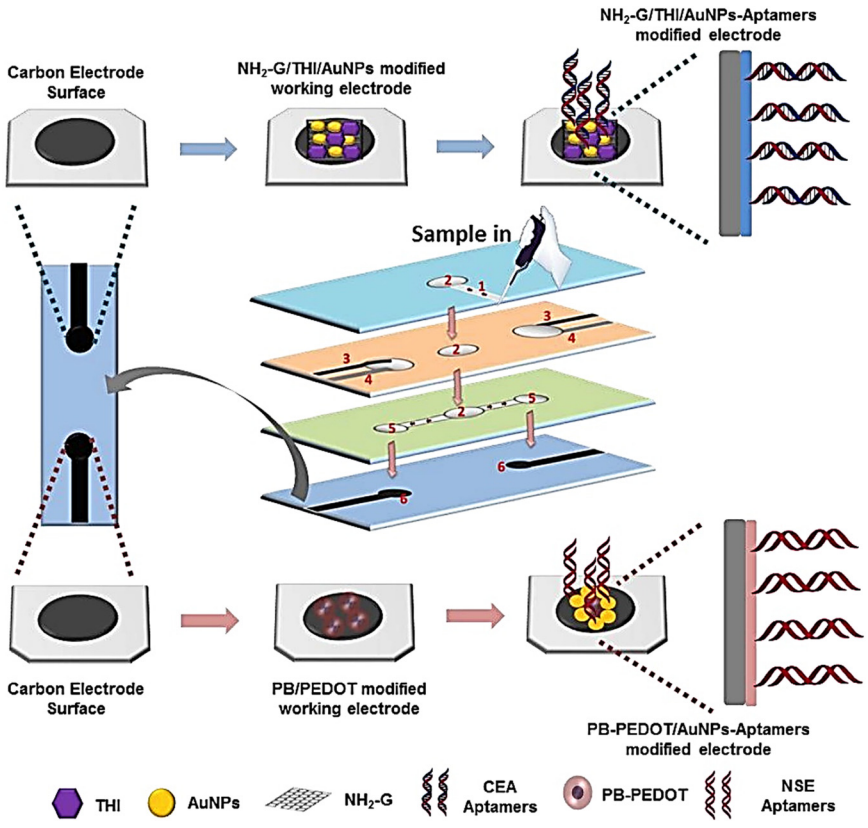

Fig. 10 Paper-based electrochemical aptasensor. The working electrode was modified using amino functional graphene (NG)–thionin (THI)–gold nanoparticles (AuNPs) and Prussian blue (PB)–poly (3,4-ethylenedioxythiophene) (PEDOT)–AuNPs nanocomposites for the immobilization of the CEA and the NSE biomarkers as well as to promote electron transfer. Figure has been adapted with permission from Wang *et al.*, Biosensors and Bioelectronics, 2019.[116]

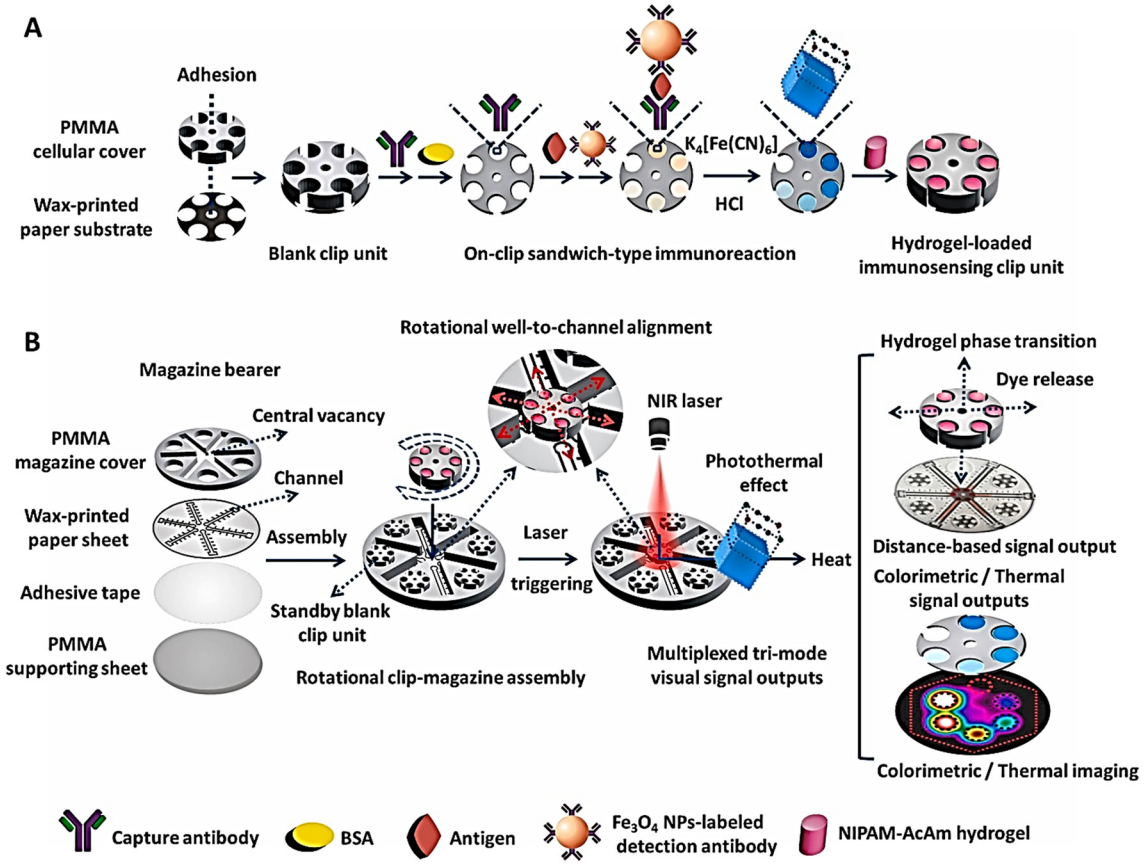

Fig. 11 A) Development of photothermal responsive hydrogel loaded poly (methyl methacrylate)/paper hybrid disk (PT-disk) based sandwich immunosensor. B) Schematic representation of the clip and magnetic bearer assembly and tri-mode visual output of immunoassay signal from the PT-disk. Figures A and B have been adapted with permission from Fu *et al.*, Biosensors and Bioelectronics, 2020.[174]

can be used to load both thermoresponsive poly(*N*-isopropylacrylamide)-acrylamide (NIPAM-AcAm) hydrogel and photothermal Fe_3O_4 nanoparticles probes. Immunocapturing of the antigen cause conversion of Fe_3O_4 to Prussian blue nanoparticles which in the presence of photothermal laser causes phase separation of the dye with the hydrogel and impart both colorimetric and thermal readout of the antigen sensing (refer to Fig. 11). Such sensors offer great versatility in portable paper-based analytical devices with visual quantitative signal readouts.[174] Overall, most of these hybrid nanomaterial-based biosensors are preclinically validated using real samples such as serum, plasma, and urine for the detection of cancer biomarkers, which enhances their possibility for further clinical validation in the future.

6. Different types of samples employed in paper-based cancer diagnosis

Applications of paper-based POC devices are generally studied using various biological samples such as blood, urine, sweat, tears, and saliva (refer to Table 2).

6.1 Blood samples

Blood has accessibility to all bodily sites, hence it can help diagnose different malignancies through abnormal tissue-specific pathological signatures. The complex nature of blood due to the presence of different kinds of cells, salts, and proteins affects the final analysis using sophisticated instruments due to volume constraints post plasma or serum separation.[175] Therefore, paper-based biosensors are employed due to minimal plasma or serum sample requirements. Microfluidic devices can diagnose breast cancer by detecting human epidermal growth factor receptor (HER2) in serum samples with a 1 pM limit of detection.[176] Similarly, μPADs employ gold nanoparticle-coated electrodes to detect cancer antigen-125 (CA-125) in blood samples for the diagnosis of ovarian cancer. Gold nanoparticles-based lateral flow assays are also developed for the detection of humoral hypercalcemia of malignancy (HHM) by sensing nanograms levels of parathyroid hormone-like hormone (PTHLH) secreting factor in human serum samples.[177] PDGF-BB and thrombin can be detected in human serum spiked samples using LFA-aptasensors.[178]

Since, the increased concentration of fibrinogen in serum samples is a biomarker of advanced hepatocellular carcinoma,

Table 2 Potential biomarkers for cancer diagnosis

Cancer	Sample	Biomarker	Ref.
Breast	Blood	HER-2 ECD, CEA, CA15-3, LAG-3, MUC1, CA125, CA27.29, BRCA1, BRCA2, NY-BR-1, ING-1, ER/PR, miRNA-17-5p, miR-155, miRNA-222, miRNA-548b-5p, miR-532-502, 5 miRNA panel (let-7b-5p, miR-122-5p, miR-146b-5p, miR-210-3p, miR-215-5p), 3 miRNA panel (miR-21-3p, miR-21-5p, miR-99a-5p)	194–203
Lung	Blood	NY-ESO-1, CEA, CA19-9, SCC, CYFRA21-1, NSE, EGFR, PD-1, CEA, KRAS, ALK (anaplastic lymphoma kinase), miR-339-5p, miR-21, miR-141, miR-145, miR-210-3p, miRNA-31, 6 miRNA panel (miR-19b-3p, miR-21-5p, miR-221-3p, miR-409-3p, miR-425-5p, miR-584-5p), 3 miRNA panel (miR-28-5p, miR-362-5p, miR-660-5p), 3 miRNA panel (miR-16, miR-205, miR-486), 4 miRNA panel (miR-146b, miR-205, miR-29c, miR-30b), 3 miRNA panel (miR-21, miR-210, miR-486-5p)	204–214
Liver	Blood	PD-1, AFP, CEA, miR-224, miRNA-200 lncRNA-TSIX, miR-548-a-3p, SOGA1, miRNA-122a, 3 miRNA panel (miR-122, miR-148a, miR-1246)	215–219
Ovarian	Blood	CA125, CA15-3, HER2, BRCA1/2, AFP, hCG, p53, CEA, CA549, CASA, CA19-9, MCA, MOV-1, TAG72, KRAS	220–222
Gastric	Blood	CEA, HER-2 ECD, LAG-3, CA72-4, CA19-9, miR-101, miRNA-22-3p, miR-196a/b, 2 miRNA panel (miR-19b-3p, miR-106a-5p), 2 miRNA panel (miR-21, miR-222), 4 miRNA panel (miR-21, miR-93, miR-106a, miR-106b), 3 miRNA panel (miR-221, miR-376c, miR-744)	223–232
Colorectal	Blood	EGFR, CEA, KRAS, miRNA-141, miR-338-5p, miR-497, 2 miRNA panel (miR-1290, miR-320d), 7 miRNA panel (miR-103a-3p, miR-127-3p, miR-151a-5p, miR-17-5p, miR-181a-5p, miR-18a-5p, miR-18b-5p), miRNA panel (miR-144-3p, miR-425-5p, miR-1260b)	233–240
Pancreatic	Blood	PD-1, CEA, CA19-9, CA125, TIM-3, KRAS, hsa-miR-21-5p, miR-221-3p, microRNA-100, miR-21-5p, miR-182, 2 miRNA panel (miRNA-196, miRNA-200 with CA19-9), 6 miRNA panel (let-7b-5p, miR-192-5p, miR-19a-3p, miR-19b-3p, miR-223-3p, miR-25-3p), 2 miRNA panel (miR-10b, miR-30c)	241–248
Bladder	Blood	BAT, FDP, NMP22, HA-Hase, BLCA-4, CYFRA 21-1, miR-155	220–222, 249
	Urine	2 miRNA panel (miR-93-5p, miR-516a-5p), 4 miRNA panel (let-7b-5p, miR-149-5p, miR-146a-5p, miR-423-5p)	250, 251
Prostate	Blood	PSA, PAP, 3 miRNA panel (miR-145, miR-148, miR-185)	221, 222, 252
Esophageal	Tumor tissue	SCC	221
	Blood	6 miRNA panel (miR-106a, miR-18a, miR-20b, miR-486-5p, miR-584, miR-223-3p)	232
Endometrial	Blood	CA 125, 6 miRNA panel (miR-143-3p, miR-195-5p, miR-20b-5p, miR-204-5p, miR-423-3p, miR-484)	222, 253
Diffuse large B-cell lymphoma (DLBCL), chronic lymphocytic leukemia (CLL)	Tumor tissue and blood	PD-L1	220
Osteosarcoma	Tumor tissue	TIM-3, miR-663a, miR-139-5p, miR-101	222, 254–256
Chronic myeloid leukemia	Blood and bone marrow	BCR-ABL1	221
Non-Hodgkin's lymphoma	Blood	let-7a, miR-124	249
Acute myeloid leukemia	Tumor tissue, blood	FLT3, IDH1/2, DNMT3A, NPM1, SRSF2, let-7a, miR-124	249, 257, 258
Melanoma	Tumor tissue	PD-1, GP100, MAGE-A, Tyrosinase, NY-ESO-1	222
Testicular	Blood	Alpha-fetoprotein (AFP), β-human chorionic gonadatropin, CAGE-1, ESO-1	221, 222
Glioma	Tumor tissue, cerebrospinal fluid	IDH1, IDH2, MGMT, PPM1D, H3F3A,	259–261
	Blood	miR-182, 3 miRNA panel (miR-19a-3p, miR-106a-5p, miR-181b-5p)	262, 263

a point-of-care paper-based biosensor to quantify plasma fibrinogen concentration has been recently developed.[179] Thrombin is added to the paper strips followed by the addition of the plasma samples containing known concentrations of fibrinogen. The reaction between thrombin and fibrinogen leads to differential eluted lengths when placed in elution baths, which is inversely correlated to the fibrinogen concentration.[180]

6.2 Urine samples

Urine is a commonly collected biological fluid for the detection of various diseases because of the presence of various analytes (proteins, cells, hormones, drugs, bilirubin, glucose, albumin, creatinine,). It has a broad pH range of 4.5–8.0 and a viscosity of 0.6–1.2 mPa s. As compared to blood, it requires fewer sample processing steps, but in a few cases, it requires

processing such as buffer dilution to remove sample turbidity and pH neutralization as urine's acidic pH might affect the reagent or antibody coated onto the paper.[181] Urine contains various cancer biomarkers such as sarcosine and citrate for prostate cancer, nuclear matrix protein number 22 (NMP22) for bladder cancer, neutrophil gelatinase-associated lipocalin (NGAL), matrix metalloproteinase 9 (MMP-9), and a disintegrin and metalloprotease-12 (ADAM-12) for breast cancer, HPV (human papillomavirus) E6 oncoprotein for cervical cancer, and perilipin-2 for renal cancer.[93,100,182,183] Therefore, plasmonic gold nano rattles coated and cysteine-capped gold nanoclusters coated paper-based microfluidic devices were explored for the detection of perilipin-2 and citrate, respectively.[93,100] A commercial paper-based OncoE6™ cervical test is also available for the detection of HPV16-E6 oncoprotein present in urine, responsible for cervical cancer.[182] Synthetic urinary biomarkers have also been reported for the paper-based detection of colorectal cancer by developing protease-sensitive peptide-coated nanoworms (NWs) with reporter probes. MMP-9 released by colorectal cancer cells cleaves the protease-sensitive linkages and facilitates the release of fluorescent probes into the urine for subsequent detection (refer to Fig. 12).[184] Despite many advantages associated with the high usage of urine samples for detection purposes, sometimes due to contamination, incorrect collection as well as presence of interfering agents can result in pre-analytical errors.[185]

6.3 Other samples

Salivary samples can be used due to the presence of various cancer biomarkers such as IL-6, IL-8, CYFRA-21-1, sCD44, *etc.*[186–189] CD44 biomarker in saliva-containing oral rinse of oral cancer patients was detected using a colorimetric lateral flow assay.[190] Saliva has also been used for the detection of cancer using various non-paper-based biosensors.[186,191] The advantages of using saliva involve its non-invasive nature along with low sample processing costs. However, the disadvantages include the chances of interference due to various other substances present in saliva such as food, mucins, bacteria, and the presence of biomarkers in lesser quantity as compared to blood or urine.[192] To detect oral and oropharyngeal cancer from oral rinses, a paper-biosensor with salivary biomarker (CD44) test strips immobilized with anti-CD44 monoclonal antibodies has been developed.[190]

Swab samples obtained from the internal lining of the wound, respiratory tract, and cervix, consisting of mucous, cancer cells or biomarkers, and other components, can also be used for cancer detection. Multiple studies have reported the paper-based detection of cervical cancer biomarkers (HPV 6, 11, 16, and 18) in cervical swabs using lateral flow assays.[67] The commercial device OncoE6™ developed for cervical cancer diagnosis through urine can also employ vaginal and cervical scrapes from the patients.[182] Detection using swabs and scrapes is an inexpensive way to collect specimens for cancer testing. However, chances of infection and patient discomfort are the major concerns.

Cancer tissues can also be directly used for diagnosis after extraction and amplification of the DNA from the tissue specimen. Klapperich *et al.* reported a colorimetric and lateral flow paper fluidic device that detects HPV 16 DNA from cervical tissue specimens.[193] In addition, various samples such as tears, sweat, and VOCs have gained major importance because of rapid analysis due to their direct usage for detection without any sample processing, but fast

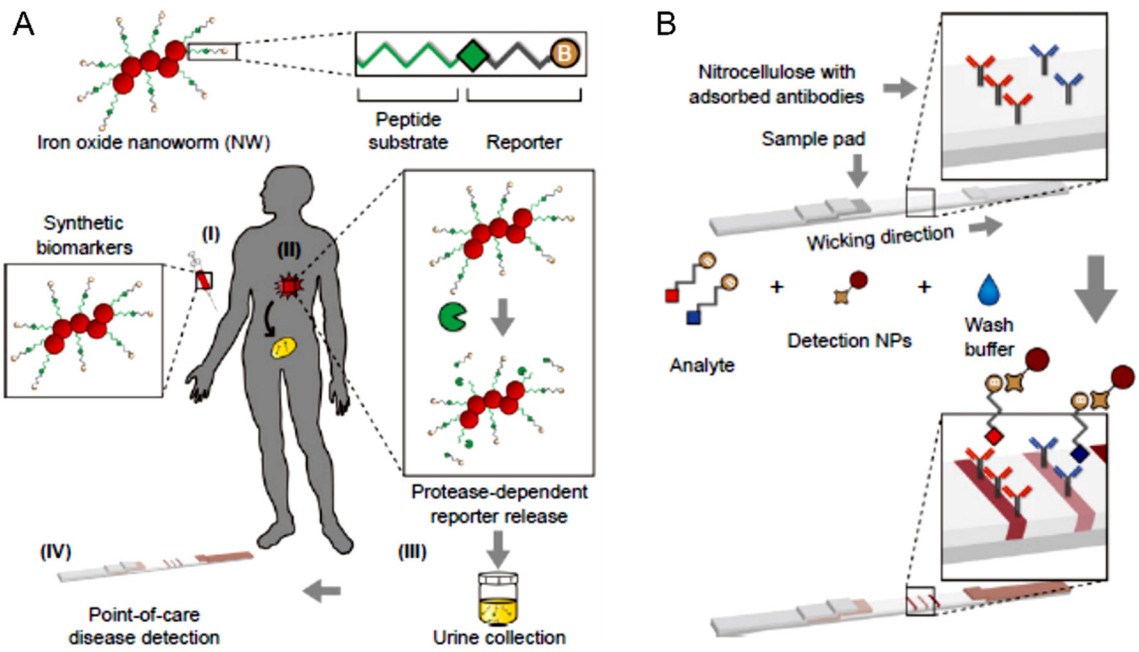

Fig. 12 Schematic of the synthetic urinary biomarker and steps involved in its *in vivo* processing to excrete detectable analyte in urine (A) and its subsequent paper-based detection (B). Figures A and B have been adapted with permission from Warren *et al.*, PNAS, 2014.[184]

evaporation and low sample volume can also lead to false results. Their application for cancer detection is majorly restricted to sophisticated techniques to date and needs further advancements. In conclusion, the selection of samples for biosensing should be dependent on factors such as a higher abundance of biomarker-of-interest, non-invasive nature of the sample collection, low cost, lesser volume, and lesser sample processing.

7. Clinical validation of paper-based cancer diagnostics

In vitro diagnostics (IVDs) are generally classified as per medical device regulatory norms. Based on the level of risk involved, cancer-specific IVDs can be categorized into class III (classification system, class I–III) according to the Food and Drug Administration (FDA, USA) and class C (classification system, class A–D) as per the European Union '*In Vitro* Diagnostic Medical Devices Regulation (IVDR)' and Central Drugs Standard Control Organization (CDSCO, India). All such devices are evaluated on their analytical performance, including biases or device inaccuracy, imprecision, analytical specificity, and sensitivity. *In vitro* diagnosis requires validation using clinical samples obtained directly from the patient to establish its efficacy. Multiple paper-based *in vitro* diagnostics are clinically approved for cancer detection.[264] Transferrin detection kit and OncoE6™ test specific for colon cancer-specific transferrin and cervical cancer-specific HPV (16 and 18) E6 oncoprotein are a few such examples (refer to Table 1).[182,265] In addition, numerous paper-based devices based on conventional and advanced approaches have been validated using clinical samples from cancer patients as a proof-of-concept. A comprehensive table of such devices has been provided below (refer to Table 3). Successful clinical translation of these devices requires strict adherence to the guidelines provided by the specific regulatory agencies.

8. Challenges and future prospects

Paper-based diagnosis has come a long way from glucose testing as a basic dipstick assay to advanced disease detection like cancer, COVID-19, *etc.* Advancements in the paper substrate, employing it in multiple assay formats along with the inclusion of advanced nanomaterial-based detection and signal enhancement techniques have enhanced the sensitivity and specificity of paper-based detection of cancer.

Although LFA allows easy detection, the laborious sample preparation and multiplex detection limit its use. VFA conquers these limitations by allowing the vertical flow of samples for enhanced interaction and multiple detections.[281] Microfluidics devices have emerged as a remarkable tool for POC detection by integrating small devices on laboratory chips with homogeneous mixing of samples.[20] The progress in screen printing of paper electrodes has offered rapid analysis at the nanoscale with high sensitivity.[281,282]

However, a few bottlenecks such as inadequate limit-of-detection, the need for an extensive pre-processing of the sample before usage, the lesser scope for quantification of signal, fewer types of detectable samples (particularly a challenge for whole cell detection), use of a single biomarker for detection, and instability of detecting biomarkers on a paper-substrate can limit their use to only primary screening in clinical settings.[37,283,284] Different approaches in terms of enhancing the device design as well as constituent detecting molecules from qualitative to quantitative detection are being explored. Upgradation of conventional qualitative assays like dot blots to quantitative formats (quantitative dot blot) and the use of newer nanomaterials (such as upconversion nanoparticles and gold nanorattles) can significantly enhance the limit-of-detection.[54,100,113] Advancements in user-friendly detection strategies like colorimetric can be achieved through the impregnation of metal–organic frameworks (MOFs) like NH2-MIL-125(Ti) in the paper or by using thermochromic fibre papers by impregnating organic dye functionalized SiO_2 nanoparticles for the photothermal detection of analytes in ng ml^{-1} range.[285,286] Visual colorimetric readouts can also be coupled with electrical output using flexible piezoelectric pressure sensors of a hybrid conductive material composed of multiwalled carbon nanotubes (MWCNTs) and polyaniline urchin-like hollow spheres (PANI-UHSs) and an elastic thermoplastic polyurethane (TPU) substrate.[287] Functionalizing paper electrodes with multiwalled carbon nanotube in a pressure-tight system can impart great sensitivity to pressure changes induced by analyte detection byproduct gas and impart good resistance with a detection limit of $<$200 pg CEA per ml.[288] Introduction of conducting paper that employs the printing of carbon-based electrodes, photoelectric materials ($NaNbO_3$ nanostructures, g-C_3N_4 quantum dots modified TiO_2 nanospheres, Bi_2O_2S (BOS) nanosheets), or conducting polymers on paper can provide a wider scope of quantification through electrochemical detection in comparison to conventional colorimetric and fluorometric strategies.[289–291] The amalgamation of such materials possessing unique properties can improve the limit of detection to even femtogram per ml. Nano-inks developed from inorganic-carbon-conducting polymer composites are one such example.[167] Miniaturization and technological advancements in the detection process by integrating mobile cameras for easy fluorescence readout instead of bulky fluorescence equipment and the development of battery-triggered electrochemiluminescence readers can be very beneficial for robust and portable applications.[276,292]

Capturing cancer-derived exosomes is an emerging way of detecting malignancies through liquid biopsies like blood or urine.[293,294] Gold nanoparticles tethered aptamer-based capturing of exosomes and multi-directional hybridization chain reaction using hairpin-like DNA unit 1/2 to recruit multiple signal molecules can enable electrochemical signal amplification and aptasensing of as low as 283 exosomes per μl of sample.[293] Nevertheless, overcoming the bottlenecks like negating the false positives by identifying the exosomes

Table 3 Examples of paper-based cancer diagnostics employing clinical samples

Type	Cancer biomarker	Cancer type	Sample	Sensing molecule	Detection technique	Sample volume	LOD	Assay time	Ref.
Dipstick	Transferrin (Tf)	Colon cancer	Patient's faeces	Transferrin test kit	Colorimetric	NR	NR	<5 min	265
	Exosomes	Hematological cancers, melanoma	Cell supernatants, plasma, urine	Gold nanoparticles	Colorimetric	100 μl	8.54 × 105 exosomes per μl	15 min	266
Lateral flow assay	HPV 16 and 18 E6 oncoprotein	Cervical cancer	Patient's urine, vaginal and cervical scrapes	OncoE6™ cervical test kits	Colorimetric	Urine (5 ml), vaginal sample (6 ml)	NR	2 ½ hours	182
	Ramos cells	B-cell, human Burkitt's lymphoma	Ramos cells spiked blood	Gold nanoparticles-aptamer conjugates	Colorimetric	80	800 Ramos cells	15 min	267
	Micro RNR's miR-210 and miR-424	Breast cancer, gastrointestinal cancer	NR	Gold nanoparticle	Colorimetric	50 μl	10 pmol	NR	268
	Alpha-fetoprotein (AFP)	Liver cancer	Patient's serum	Gold nanoparticle	Colorimetric	100 μl	0.1 ng ml^{-1}	10 min	269
	HPV-16 & HPV-18 DNA	Cervical cancer	Patient's plasma	CRISPR–Cas12a	Fluorescence	25 μl	0.24fM	3 hours	70
	Parathyroid hormone-like hormone	Humoral hypercalcemia of malignancy	Patient's serum	Gold nanoparticles	Fluorescence	150 μL	1.42 ng ml^{-1}	15–20 min	177
	Carbohydrate antigen CA19-9	Pancreatic and colorectal cancer	Patient's plasma	Antibody conjugated gold nanoparticles	Colorimetric	100 μL	5 U ml^{-1}	5 min	270
	Perilipin-2 (PLIN-2)	Renal cancer	Patient's urine	Anti-PLIN-2 linked gold nanorattles	Localized surface plasmon resonance	Few drops of urine	NR	2 hours	100
	HPV DNA	Cervical cancer	Patient's cervical tissue	Antibody against amplified DNA	Colorimetric	6 μL	10^4 DNA copies	1 hour	193
	CD44	Oral cancer	Patient's oral rinses	Antibody against sCD44	Colorimetric	5 mL	NR	10 min	190
	HPV 6, 11, 16, and 18 DNA	Cervical cancer	Patient's cervical tissue swabs	Fluorescently labelled DNA	Fluorescence	5 μL	10–102 plasmid DNA per μL	30 min	67
	Volatile benzaldehyde	Lung cancer	Patient exhaled breath	Gold nanorods and quantum dots embedded metal organic framework structures (GNRs-QDs@NU-901)	Fluorescence and SERS signal	1000 mL (~500 mL × 2)	1.2–0.1 ppb	5 min	110
Vertical flow assay	CEA, alpha-fetoprotein (AFP), Cancer antigen 199	Multiple cancer types	Patient's serum	FITC labelled anti-CEA, anti-AFP, anti-CA199 antibodies	Fluorescence	10 μL	CEA (0.03 ng ml^{-1}), AFP (0.05 ng ml^{-1}), CA199 (0.09 ng ml^{-1})	220 s	38
	Prostate-specific antigen (PSA), CEA, AFP	Prostate cancer	Patient's serum	Raman dyes (RDs) encoded core–shell SERS nanotags	Fluorescence	30 μL	0.37, 0.43, and 0.26 pg ml^{-1} for PSA, CEA, and AFP	7 min	39
μPADs	Cancer antigen (CA-125)	Ovarian cancer	Patient's blood	Gold nanoparticles	Electro-chemical	5 μl	3500 U ml^{-1}	NR	49
	CA-125	Ovarian cancer	CA-125 spiked	Silver nanoparticles/reduced	Electro-chemical	10 μl	0.78 U ml^{-1}	1	166

Table 3 *(continued)*

Type	Cancer biomarker	Cancer type	Sample	Sensing molecule	Detection technique	Sample volume	LOD	Assay time	Ref.
			human plasma	graphene oxide (Ag/RGO) nano-ink and cysteamine caped gold nanoparticles (CysA/Au NPs)				hour	
	DNA sequences	Chronic myelogenous leukemia	Patient's blood	Cadmium selenide quantum dots with complementary DNA probes	Electro-chemical	NR	10^{-15} M	NR	271
	CEA, Her-2/Neu (C-erbB-2)	Colon and breast cancer	Patient's serum and saliva	CdSe/ZnS quantum dots bio-conjugated labels	Fluorescent	NR	CEA (0.02 ng ml^{-1}), Her2/Neu (0.27 ng ml^{-1})	27 min	272
	273	Oral Cancer	Patient's saliva	G-rich target recognition sequence attached onto gold electrode	Electro-chemical	5 μl	0.02 fM	1.5–2 hours	273
	miRNA 21	Breast cancer	Patient's blood	Molecular beacon probes	Fluorescence	50 μl	0.01 μM	30 min	274
	AFP, CEA, carbohydrate antigen 125 (CA125), CA153	Colon, lung, ovarian, pancreatic, liver and breast cancer	Patient's serum	Antibody coated graphene and chitosan modified screen printed paper electrode	Electro-chemical	2.0 μL	0.005 ng ml^{-1}	5 min	275
	PSA, CEA	Prostate, colon, lung, ovarian, pancreatic, liver and breast cancer	Patient's serum	Antibody linked graphene oxide-chitosan/AuNPs nanocomposite coated on screen printed paper electrode	Electro-chemiluminescence	4.0 μL	0.8 pg ml^{-1}	15 min	276
	ROR1+ cancer cells	Haematological cancer (chronic lymphocytic leukemia, B-cell acute lymphoblastic leukemia)	Buffy coat blood samples	Antibody-conjugated fluorescent microparticles	Fluorescence	10 μL	0.1 cells per μl	<10 min	277
	Thioredoxin-1	Breast cancer	Blood serum samples	Anti-Trx-1 antibody-conjugated with HRP	Colorimetric	100 μL	0–200 ng ml^{-1}	14 min	50
Conducting paper electrodes	CEA	Colorectal, lung, gastric, pancreatic, cervical cancer	Patient's serum	Anti-CEA linked graphene/thionine/gold nanoparticles (AuNPs) nocomposite coated on screen printed paper electrode	Electro-chemical	NR	10 pg ml^{-1}	NR	82
	CA 125 antigen	Ovarian cancer	CA 125 spiked in p plasma	Ag–DPA–GQD/CysA–Au NPs Cysteamine coped gold nanoparticles (CysA/Au NPS)	Electro-chemical	NR	15 U ml^{-1}	2 min	278
	Cancer antigen 125 (CA125)	Ovarian cancer	Patient's serum	Antibody tagged nanocomposites (reduced graphene oxide/thionine/AuNPs)	Electro-chemical	NR	0.01 U ml^{-1}	20 min	279
	Human epidermal growth factor receptor (HER2)	Breast cancer	HER2 spiked undiluted serum	Aptamers immobilized on gold micro-electrode arrays on silicon/-silicon oxide wafers	Electro-chemical	50 μl	1 pM	30 min	176
	CEA	Colon, lung, ovarian, pancreatic, liver and breast cancer	Patient's serum	Anti-CEA taggedPEDOT:PSS – CNT nanocomposite	Electro-chemical	NR	2 ng ml^{-1}	15 min	164
	CEA	Colon, lung, ovarian, pancreatic, liver and breast cancer	Patient's serum	Anti-CEA tagged PEDOT:PSS – iron oxide (Fe_2O_3) nanocomposite	Electro-chemical	NR	4 ng ml^{-1}	10 min	165
	CEA	Colon, lung, ovarian, pancreatic, liver and breast	Patient's serum	Anti-CEA tagged reduced graphene oxide (rGO)	Electro-chemical	10 μl	1 ng ml^{-1}	20 s	280

Table 3 *(continued)*

Type	Cancer biomarker	Cancer type	Sample	Sensing molecule	Detection technique	Sample volume	LOD	Assay time	Ref.
		cancer							
	CEA	Colon, lung, ovarian, pancreatic, liver and breast cancer	Patient's serum	Anti-CEA tagged PEDOT:PSS – polyvinyl alcohol nanofibers	Electro-chemical	10 μL	0.2 ng ml^{-1}	10 min	162
	AFP	Hepatocellular carcinoma	Patient's serum	Antibody linked branched zinc nanorods modified rGO	Electro-chemical	20 μL	0.08 pg ml^{-1}	10 min	172
	PSA	Prostate cancer	Patient's serum	Antibody linked gold nanorods	Electro-chemical	5.0 μL	1.5 pg ml^{-1}	1.5 hours	101
	CYFRA 21-1	Lung Cancer	Patient's blood	Phthalocyanine-BODIPY dye	Electro-chemical	1 mL	0.20 pg ml^{-1}	10 min	86

secreted by normal cells, reduction of sample volume, and exosome stability during analysis would help unleash the true potential of these biosensors for clinical sample analysis.[295] Genetic biomarker sensing would be extremely important for personalized cancer treatment, therefore, detecting cancer-specific genetic biomarkers like the BRCA1 gene from breast or ovarian cancer patients, methylguanine methyl transferase (MGMT), IDH1/2 from glioma patients, FLT3, DNMT3A from acute myeloid leukemia, *etc.* would be the way forward to develop next-generation paper-based diagnostics.[296,297] Electrochemical biosensors can be tuned to detect the BRCA1 mutated cancer patients by capturing BRCA1 single-stranded DNA (ssDNA) using complementary DNA adhered lipid membrane-coated gold nanoparticles. Anchoring this complex onto a 2D-layer of graphene analogue *i.e.* MXene can several fold enhance the ssDNA detection signal and increase the limit of detection to 1zM (zeptomolar).[298] Electrochemical-based biosensing of biomarker DNA up to 1.2 pM can be achieved by integrating CRISPR–Cas12a in a portable biosensor with a smartphone-based signal read for resource-limiting conditions. Semiconductors like In_2O_3–In_2S_3 can be used to modify the paper substrate for photoactivation, which can generate photocurrents based on differential G-quadruplexes cleavage by activated target DNA-bound CRIPR–Cas12a.[72]

To make these biosensors more user-friendly and compact, research is being driven toward making 'all-in-one' paper-based devices. It focuses on capturing and amplifying target nucleic acid present in the sample directly on paper and integrating it with the detection system using paper fluidics.[193] Paper fluidics approach can reduce the detection time to 1 hour and also open the doors to capture more varied types of 'biomarkers' on paper, for instance, capturing cancerous cells directly.[193,277] Since the conventional biorecognition elements such as antibodies, DNA, and PNA, are relatively less stable on paper-substrate, new bio-recognition elements such as synthetically injectable and tunable markers and MIPs are gaining importance.[75,184] In addition, research focuses on modifying the paper substrate itself through the generation of nitrocellulose–polymer composites can also address the above-mentioned limitations, including the requirement of flexible substrates to capture intact cells and the printing of electrodes for enhanced detection.[5,299] All these new strategies have shown promising results as a proof-of-concept, however, the efficacy of these paper-based techniques as point-of-care diagnostics will truly be validated upon testing in a large cohort of patients in clinical trials and real-world settings. Overall, paper-based sensors offer promising future applications in personalized therapy for cancer by enabling: real-time monitoring of disease biomarkers and treatment responses, facilitating immediate adjustments to therapy, augmenting precision medicine approaches through personalized molecular profiling and targeted therapy selection, and early detection of disease recurrence or treatment resistance. Integration of data analytics and machine learning to the paper-based cancer biosensing can tremendously help identify clinical biomarkers, their rapid and

minimally invasive detection, and provide personalized therapy decisions in a highly cost-effective manner.[300]

Author contributions

Prateek Bhardwaj: conceptualization, investigation, project administration, supervision, validation, visualization, writing – original draft, writing – review & editing. Survanshu Saxena: investigation, writing – original draft. Bharti Arora: investigation, writing – original draft. Subhasini Singh: investigation, writing – original draft. Pranoti Palkar: investigation, writing – review & editing. Rinti Banerjee: supervision, resources. Jayant Sastri Gota: supervision, validation, resources, writing – review & editing.

Conflicts of interest

The authors declare no conflict of interests.

Acknowledgements

All the authors would like to acknowledge Prof. Rinti Banerjee (whom we lost during COVID-19 pandemic) for her guidance and scientifically grooming early career researchers like Dr. Prateek Bhardwaj, Survanshu Saxena, Bharti Arora, and Subhasini Singh.

References

1 N. Emrizal, Z. Mohd Zain and K. G. Heah, *Asia-Pac. J. Mol. Biol. Biotechnol.*, 2023, **31**(2), 62–70.
2 K. J. Land, S. Smith and R. W. Peeling, in *Paper-based Diagnostics: Current Status and Future Applications*, ed. K. J. Land, Springer International Publishing, Cham, 2019, pp. 1–21, DOI: **10.1007/978-3-319-96870-4_1**.
3 M. Sher, R. Zhuang, U. Demirci and W. Asghar, *Expert Rev. Mol. Diagn.*, 2017, **17**, 351–366.
4 K. Ratajczak and M. Stobiecka, *Carbohydr. Polym.*, 2020, **229**, 115463.
5 H. Shafiee, W. Asghar, F. Inci, M. Yuksekkaya, M. Jahangir, M. H. Zhang, N. G. Durmus, U. A. Gurkan, D. R. Kuritzkes and U. Demirci, *Sci. Rep.*, 2015, **5**, 8719.
6 B. Asci Erkocyigit, O. Ozufuklar, A. Yardim, E. Guler Celik and S. Timur, *Biosensors*, 2023, **13**(3), 387.
7 A. Dukle, A. J. Nathanael, B. Panchapakesan and T.-H. Oh, *Biosensors*, 2022, **12**(9), 737.
8 C. Pereira, C. Parolo, A. Idili, R. R. Gomis, L. Rodrigues, G. Sales and A. Merkoçi, *Trends Chem.*, 2022, **4**, 554–567.
9 A. A. Shalaby, C.-W. Tsao, A. Ishida, M. Maeki and M. Tokeshi, *Sens. Actuators, B*, 2023, **379**, 133243.
10 M. Y. Azab, M. F. O. Hameed and S. S. A. Obayya, *Biology*, 2023, **12**, 232.
11 K. Ratajczak and M. Stobiecka, *Carbohydr. Polym.*, 2020, **229**, 115463.
12 N. Yonet-Tanyeri, B. Z. Ahlmark and S. R. Little, *Adv. Mater. Technol.*, 2021, **6**(8), 2001138.
13 R. H. Tang, M. Li, L. N. Liu, S. F. Zhang, N. Alam, M. You, Y. H. Ni and Z. D. Li, *Cellulose*, 2020, **27**, 3835–3846.
14 X. Deng, N. M. Smeets, C. Sicard, J. Wang, J. D. Brennan, C. D. Filipe and T. Hoare, *J. Am. Chem. Soc.*, 2014, **136**, 12852–12855.
15 C. T. Yew, P. Azari, J. R. Choi, F. Li and B. Pingguan-Murphy, *Anal. Chim. Acta*, 2018, **1009**, 81–88.
16 K. Kim, H. A. Joung, G. R. Han and M. G. Kim, *Biosens. Bioelectron.*, 2016, **85**, 422–428.
17 J. A. Jenkins, L. Dube, Y. Luo, J. Chen, T. H. Fan, Y. Lei and J. Zhao, *Sens. Actuators, B*, 2018, **262**, 493–498.
18 S. S. Acimovic, M. A. Ortega, V. Sanz, J. Berthelot, J. L. Garcia-Cordero, J. Renger, S. J. Maerkl, M. P. Kreuzer and R. Quidant, *Nano Lett.*, 2014, **14**, 2636–2641.
19 T. Brandstetter, S. Bohmer, O. Prucker, E. Bisse, A. zur Hausen, J. Alt-Morbe and J. Ruhe, *J. Virol. Methods*, 2010, **163**, 40–48.
20 A. K. Yetisen, M. S. Akram and C. R. Lowe, *Lab Chip*, 2013, **13**, 2210–2251.
21 M. F. Syful Azlie, M. R. Hassan, S. Junainah and B. Rugayah, *Med. J. Malays.*, 2015, **70**, 24–30.
22 S. Wang, X. Wang, S. Tang, Y. Chen, J. Jia, J. Chen, H. Shen and B. Bai, *Lab. Med.*, 2019, **50**, 130–137.
23 A. T. Singh, D. Lantigua, A. Meka, S. Taing, M. Pandher and G. Camci-Unal, *Sensors*, 2018, **18**(9), 2838.
24 K. M. Koczula and A. Gallotta, *Essays Biochem.*, 2016, **60**, 111–120.
25 B. W. Liu, D. Du, X. Hua, X. Y. Yu and Y. H. Lin, *Electroanalysis*, 2014, **26**, 1214–1223.
26 **https://ctkbiotech.com/products/?filters=product_cat[biomarkers-rapid-tests]**.
27 **https://www.alere.com/en/home/products-services/product-lookup.html**.
28 **https://www.arborvita.com/avproducts/**.
29 **https://www.quickingbio.com/**.
30 **https://www.bio-techne.com/diagnostics/lateral-flow-assay-development**.
31 **https://www.rapidtest.com/index.php/Tabs/tabs/index.php?product=Cancer-Rapid-tests&cat=22**.
32 **https://www.lifesignmed.com/product-catalog/urology/status-bta**.
33 **https://www.alfascientific.com/products/**.
34 **https://www.accubiotech.com/category?catid=2**.
35 **https://www.turklab.com.tr/products/product-list**.
36 **https://www.ultimed.org/produktkategorie/rapid-tests/**.
37 N. Jiang, R. Ahmed, M. Damayantharan, B. Unal, H. Butt and A. K. Yetisen, *Adv. Healthcare Mater.*, 2019, **8**, e1900244.
38 Y. C. Jiao, C. Du, L. J. Zong, X. Y. Guo, Y. F. Han, X. P. Zhang, L. Li, C. W. Zhang, Q. Ju, J. H. Liu, H. D. Yu and W. Huang, *Sens. Actuators, B*, 2020, **306**, 127239.
39 R. Chen, B. Liu, H. Ni, N. Chang, C. Luan, Q. Ge, J. Dong and X. Zhao, *Analyst*, 2019, **144**, 4051–4059.
40 F. A. Vicente, I. Plazl, S. P. M. Ventura and P. Znidarsic-Plazl, *Green Chem.*, 2020, **22**, 4391–4410.
41 G. Luka, A. Ahmadi, H. Najjaran, E. Alocilja, M. DeRosa, K. Wolthers, A. Malki, H. Aziz, A. Althani and M. Hoorfar, *Sensors*, 2015, **15**, 30011–30031.

42 B. Alsaeed and F. R. Mansour, *Microchem. J.*, 2020, **155**, 104664.
43 A. W. Martinez, S. T. Phillips, M. J. Butte and G. M. Whitesides, *Angew. Chem., Int. Ed.*, 2007, **46**, 1318–1320.
44 C. Özyurt, İ. Uludağ, B. İnce and M. K. Sezgintürk, *J. Pharm. Biomed. Anal.*, 2023, **226**, 115266.
45 C. M. Pandey, S. Augustine, S. Kumar, S. Kumar, S. Nara, S. Srivastava and B. D. Malhotra, *Biotechnol. J.*, 2018, **13**, 1700047.
46 C. Baynes and J. Y. Yoon, *SLAS Technol.*, 2018, **23**, 30–43.
47 P. Lisowski and P. K. Zarzycki, *Chromatographia*, 2013, **76**, 1201–1214.
48 E. Lazzarini, A. Pace, I. Trozzi, M. Zangheri, M. Guardigli, D. Calabria and M. Mirasoli, *Biosensors*, 2022, **12**, 825.
49 B. B. Nunna, D. Mandal, J. U. Lee, H. Singh, S. Zhuang, D. Misra, M. N. U. Bhuyian and E. S. Lee, *Nano Convergence*, 2019, **6**, 3.
50 M. J. Lee, V. Soum, S. N. Lee, J. H. Choi, J. H. Shin, K. Shin and B. K. Oh, *Anal. Bioanal. Chem.*, 2022, **414**, 3219–3230.
51 Z. Z. Shi, Y. Lu and L. Yu, in *Next Generation Point-of-care Biomedical Sensors Technologies for Cancer Diagnosis*, ed. P. Chandra, Y. N. Tan and S. P. Singh, Springer Singapore, Singapore, 2017, pp. 365–396, DOI: **10.1007/978-981-10-4726-8_16**.
52 X. Zhang, G. Soori, T. J. Dobleman and G. G. Xiao, *Expert Rev. Mol. Diagn.*, 2014, **14**, 97–106.
53 Q. Q. Zhuang, H. H. Deng, S. B. He, H. P. Peng, Z. Lin, X. H. Xia and W. Chen, *ACS Appl. Mater. Interfaces*, 2019, **11**, 31729–31734.
54 G. Tian, F. Tang, C. Yang, W. Zhang, J. Bergquist, B. Wang, J. Mi and J. Zhang, *Oncotarget*, 2017, **8**, 58553–58562.
55 W. Zhang, G. Yu, Y. Zhang, F. Tang, J. Lv, G. Tian, Y. Zhang, J. Liu, J. Mi and J. Zhang, *Anal. Biochem.*, 2019, **576**, 42–47.
56 X. Jiang and P. B. Lillehoj, *Analyst*, 2021, **146**, 1084–1090.
57 L. Sadaow, O. Sanpool, R. Rodpai, H. Yamasaki, W. Ittiprasert, V. H. Mann, P. J. Brindley, W. Maleewong and P. M. Intapan, *Am. J. Trop. Med. Hyg.*, 2019, **101**, 1156–1160.
58 L. M. Tian, S. Tadepalli, S. H. Park, K. K. Liu, J. J. Morrissey, E. D. Kharasch, R. R. Naik and S. Singamaneni, *Biosens. Bioelectron.*, 2014, **59**, 208–215.
59 U. H. Yildiz, P. Alagappan and B. Liedberg, *Anal. Chem.*, 2013, **85**, 820–824.
60 S. J. Chen, C. I. Rai, S. C. Wang and Y. C. Chen, *Diagnostics*, 2023, **13**, 2255.
61 P. Teengam, N. Nisab, N. Chuaypen, P. Tangkijvanich, T. Vilaivan and O. Chailapakul, *Biosens. Bioelectron.*, 2021, **189**, 113381.
62 X. Cao, Q. Song, Y. Sun, Y. Mao, W. Lu and L. Li, *Nanotechnology*, 2021, **32**, 445101.
63 B. D. Grant, C. A. Smith, P. E. Castle, M. E. Scheurer and R. Richards-Kortum, *Vaccine*, 2016, **34**, 5656–5663.
64 B. Ma, J. Fang, W. Lin, X. Yu, C. Sun and M. Zhang, *Anal. Bioanal. Chem.*, 2019, **411**, 7451–7460.
65 R. Kumvongpin, P. Jearanaikoon, C. Wilailuckana, N. Sae-Ung, P. Prasongdee, S. Daduang, M. Wongsena, P. Boonsiri, W. Kiatpathomchai, S. S. Swangvaree, A. Sandee and J. Daduang, *Mol. Med. Rep.*, 2017, **15**, 3203–3209.
66 Y. B. Kuo, Y. S. Li and E. C. Chan, *J. Virol. Methods*, 2015, **212**, 8–11.
67 Y. Xu, Y. Liu, Y. Wu, X. Xia, Y. Liao and Q. Li, *Anal. Chem.*, 2014, **86**, 5611–5614.
68 K. Dhama, K. Karthik, S. Chakraborty, R. Tiwari, S. Kapoor, A. Kumar and P. Thomas, *Pak. J. Biol. Sci.*, 2014, **17**, 151–166.
69 M. Redman, A. King, C. Watson and D. King, *Arch. Dis. Child.: Educ. Pract. Ed.*, 2016, **101**, 213–215.
70 J. H. Tsou, Q. Leng and F. Jiang, *Transl. Oncol.*, 2019, **12**, 1566–1573.
71 Z. O. Uygun, L. Yeniay and N. S. F. Gi Rgi, *Anal. Chim. Acta*, 2020, **1121**, 35–41.
72 R. Zeng, H. Gong, Y. Li, Y. Li, W. Lin, D. Tang and D. Knopp, *Anal. Chem.*, 2022, **94**, 7442–7448.
73 Y. Wu, P. Xue, K. M. Hui and Y. Kang, *Biosens. Bioelectron.*, 2014, **52**, 180–187.
74 P. Kaewarsa, T. Vilaivan and W. Laiwattanapaisal, *Anal. Chim. Acta*, 2021, **1186**, 339130.
75 G. Selvolini and G. Marrazza, *Sensors*, 2017, **17**, 718.
76 J. Qi, B. Li, N. Zhou, X. Wang, D. Deng, L. Luo and L. Chen, *Biosens. Bioelectron.*, 2019, **142**, 111533.
77 S. M. Tawfik, M. R. Elmasry, M. Sharipov, S. Azizov, C. H. Lee and Y. I. Lee, *Biosens. Bioelectron.*, 2020, **160**, 112211.
78 G. V. Martins, A. C. Marques, E. Fortunato and M. G. F. Sales, *Sens. Bio-Sens. Res.*, 2020, **28**, 100333.
79 A. R. Cardoso, M. H. de Sa and M. G. F. Sales, *Bioelectrochemistry*, 2019, **130**, 107287.
80 L. Syedmoradi, M. Daneshpour, M. Alvandipour, F. A. Gomez, H. Hajghassem and K. Omidfar, *Biosens. Bioelectron.*, 2017, **87**, 373–387.
81 E. Solhi, M. Hasanzadeh and P. Babaie, *Anal. Methods*, 2020, **12**, 1398–1414.
82 Y. Wang, H. Xu, J. Luo, J. Liu, L. Wang, Y. Fan, S. Yan, Y. Yang and X. Cai, *Biosens. Bioelectron.*, 2016, **83**, 319–326.
83 S. Kumar, S. Kumar, C. M. Pandey and B. D. Malhotra, *J. Phys.: Conf. Ser.*, 2016, **704**, 1900041.
84 Y. K. Yen, C. H. Chao and Y. S. Yeh, *Sensors*, 2020, **20**, 1372.
85 S. Kumar, S. Kumar, S. Srivastava, B. K. Yadav, S. H. Lee, J. G. Sharma, D. C. Doval and B. D. Malhotra, *Biosens. Bioelectron.*, 2015, **73**, 114–122.
86 R. I. Stefan-van Staden, I. R. Comnea-Stancu, H. Yanik, M. Goksel, A. Alexandru and M. Durmus, *Anal. Bioanal. Chem.*, 2017, **409**, 6195–6203.
87 S. Boonkaew, A. Yakoh, N. Chuaypen, P. Tangkijvanich, S. Rengpipat, W. Siangproh and O. Chailapakul, *Biosens. Bioelectron.*, 2021, **193**, 113543.
88 S. M. Park, A. Aalipour, O. Vermesh, J. H. Yu and S. S. Gambhir, *Nat. Rev. Mater.*, 2017, **2**, 17014.
89 G. Chen, I. Roy, C. Yang and P. N. Prasad, *Chem. Rev.*, 2016, **116**, 2826–2885.
90 K. Khalid, X. Tan, H. F. Mohd Zaid, Y. Tao, C. Lye Chew, D. T. Chu, M. K. Lam, Y. C. Ho, J. W. Lim and L. Chin Wei, *Bioengineered*, 2020, **11**, 328–355.
91 X. P. Huang, Y. F. Zhu and E. Kianfar, *J. Mater. Res. Technol.*, 2021, **12**, 1649–1672.

92 S. Medici, M. Peana, D. Coradduzza and M. A. Zoroddu, *Semin. Cancer Biol.*, 2021, **76**, 27–37.
93 S. Abarghoei, N. Fakhri, Y. S. Borghei, M. Hosseini and M. R. Ganjali, *Spectrochim. Acta, Part A*, 2019, **210**, 251–259.
94 L. M. Yang, M. Cui, Y. P. Zhang, L. Jiang, H. Y. Liu and Z. Liu, *Sens. Actuators, B*, 2022, **350**, 130857.
95 Q. Zhang, H. H. Yan, C. Ru, F. Zhu, H. Y. Zou, P. F. Gao, C. Z. Huang and J. Wang, *Biosens. Bioelectron.*, 2022, **201**, 113942.
96 M. Alagiri, P. Rameshkumar and A. Pandikumar, *Microchim. Acta*, 2017, **184**, 3069–3092.
97 A. Khoshroo, A. Fattahi and L. Hosseinzadeh, *J. Electroanal. Chem.*, 2022, **910**, 116182.
98 Y. K. Yen, C. H. Chao and Y. S. Yeh, *Sensors*, 2020, **20**, 1372.
99 M. Gutierrez-Capitan, A. Baldi and C. Fernandez-Sanchez, *Sensors*, 2020, **20**, 967.
100 R. Hu, R. Gupta, Z. Wang, C. Wang, H. Sun, S. Singamaneni, E. D. Kharasch and J. J. Morrissey, *Kidney Int.*, 2019, **96**, 1417–1421.
101 G. Q. Sun, H. Y. Liu, Y. Zhang, J. H. Yu, M. Yan, X. R. Song and W. X. He, *New J. Chem.*, 2015, **39**, 6062–6067.
102 W. P. Li, L. Li, M. Li, J. H. Yu, S. G. Ge, M. Yan and X. R. Song, *Chem. Commun.*, 2013, **49**, 9540–9542.
103 M. Pavithra, S. Muruganand and C. Parthiban, *Sens. Actuators, B*, 2018, **257**, 496–503.
104 J. Upan, N. Youngvises, A. Tuantranont, C. Karuwan, P. Banet, P. H. Aubert and J. Jakmunee, *Sci. Rep.*, 2021, **11**, 13969.
105 W.-J. Liu, L.-J. Wang and C.-Y. Zhang, *Anal. Chim. Acta*, 2023, **1278**, 341615.
106 M. Garcia-Cortes, J. R. Encinar, J. M. Costa-Fernandez and A. Sanz-Medel, *Biosens. Bioelectron.*, 2016, **85**, 128–134.
107 S. Bock, J. An, H. M. Kim, J. Kim, H. S. Jung, X. H. Pham, W. Y. Rho and B. H. Jun, *Bull. Korean Chem. Soc.*, 2020, **41**, 989–993.
108 Z. Lin, S. Lv, K. Zhang and D. Tang, *J. Mater. Chem. B*, 2017, **5**, 826–833.
109 Z. Qiu, J. Shu and D. Tang, *Anal. Chem.*, 2017, **89**, 5152–5160.
110 Z. Xia, D. Li and W. Deng, *Anal. Chem.*, 2021, **93**, 4924–4931.
111 J. Wang, T. Sheng, X. Zhu, Q. Li, Y. Wu, J. Zhang, J. Liu and Y. Zhang, *Mater. Chem. Front.*, 2021, **5**, 1743–1770.
112 K. Li, E. Hong, B. Wang, Z. Wang, L. Zhang, R. Hu and B. Wang, *Photodiagn. Photodyn. Ther.*, 2019, **25**, 177–192.
113 S. Xu, B. Dong, D. Zhou, Z. Yin, S. Cui, W. Xu, B. Chen and H. Song, *Sci. Rep.*, 2016, **6**, 23406.
114 H. He, B. Liu, S. Wen, J. Liao, G. Lin, J. Zhou and D. Jin, *Anal. Chem.*, 2018, **90**, 12356–12360.
115 D. Maiti, X. Tong, X. Mou and K. Yang, *Front. Pharmacol.*, 2018, **9**, 1401.
116 Y. Wang, J. Luo, J. Liu, S. Sun, Y. Xiong, Y. Ma, S. Yan, Y. Yang, H. Yin and X. Cai, *Biosens. Bioelectron.*, 2019, **136**, 84–90.
117 L. L. Liang, M. Su, L. Li, F. F. Lan, G. X. Yang, S. G. Ge, J. H. Yu and X. R. Song, *Sens. Actuators, B*, 2016, **229**, 347–354.
118 Y. Fan, S. Y. Shi, J. S. Ma and Y. H. Guo, *Biosens. Bioelectron.*, 2019, **135**, 1–7.
119 K. S. Prasad, X. Y. Cao, N. Gao, Q. J. Jin, S. T. Sanjay, G. Henao-Pabon and X. J. Li, *Sens. Actuators, B*, 2020, **305**, 127516.
120 B. Wei, K. Mao, N. Liu, M. Zhang and Z. G. Yang, *Biosens. Bioelectron.*, 2018, **121**, 41–46.
121 G. Q. Sun, L. N. Zhang, Y. Zhang, H. M. Yang, C. Ma, S. G. Ge, M. Yan, J. H. Yu and X. R. Song, *Biosens. Bioelectron.*, 2015, **71**, 30–36.
122 L. Li, L. Zhang, J. Yu, S. Ge and X. Song, *Biosens. Bioelectron.*, 2015, **71**, 108–114.
123 J. Zhou, Y. Zheng, J. Liu, X. Bing, J. Hua and H. Zhang, *J. Pharm. Biomed. Anal.*, 2016, **117**, 333–337.
124 M. Hasanzadeh and N. Shadjou, *Mater. Sci. Eng., C*, 2017, **71**, 1313–1326.
125 V. Serafin, A. Valverde, M. Garranzo-Asensio, R. Barderas, S. Campuzano, P. Yanez-Sedeno and J. M. Pingarron, *Microchim. Acta*, 2019, **186**, 411.
126 Y. Koo, V. N. Shanov and Y. Yun, *Micromachines*, 2016, **7**, 72.
127 P. Nguyen-Tri, T. A. Nguyen, P. Carriere and C. Ngo Xuan, *Int. J. Corros.*, 2018, **2018**, 4749501.
128 D. C. Ferrier and K. C. Honeychurch, *Biosensors*, 2021, **11**, 486.
129 S. Ji, M. Lee and D. Kim, *Biosens. Bioelectron.*, 2018, **102**, 345–350.
130 N. Aliakbarinodehi, G. De Micheli and S. Carrara, *Anal. Chem.*, 2016, **88**, 9347–9350.
131 F. Liu, W. Deng, Y. Zhang, S. Ge, J. Yu and X. Song, *Anal. Chim. Acta*, 2014, **818**, 46–53.
132 E. Sanchez-Tirado, A. Gonzalez-Cortes, P. Yanez-Sedeno and J. M. Pingarron, *Biosens. Bioelectron.*, 2018, **113**, 88–94.
133 H. V. Tran, B. Piro, S. Reisberg, L. D. Tran, H. T. Duc and M. C. Pham, *Biosens. Bioelectron.*, 2013, **49**, 164–169.
134 Q. M. Feng, J. B. Pan, H. R. Zhang, J. J. Xu and H. Y. Chen, *Chem. Commun.*, 2014, **50**, 10949–10951.
135 K. M. Tsoi, Q. Dai, B. A. Alman and W. C. Chan, *Acc. Chem. Res.*, 2013, **46**, 662–671.
136 S. Nikazar, V. S. Sivasankarapillai, A. Rahdar, S. Gasmi, P. S. Anumol and M. S. Shanavas, *Biophys. Rev.*, 2020, **12**, 703–718.
137 R. Bilan, I. Nabiev and A. Sukhanova, *ChemBioChem*, 2016, **17**, 2103–2114.
138 K. D. Wegner and N. Hildebrandt, *Chem. Soc. Rev.*, 2015, **44**, 4792–4834.
139 A. Singh, M. Bezuidenhout, N. Walsh, J. Beirne, R. Felletti, S. Wang, K. T. Fitzgerald, W. M. Gallagher, P. Kiely and G. Redmond, *Nanotechnology*, 2016, **27**, 305603.
140 X. Zhang, J. Yu, C. Wu, Y. Jin, Y. Rong, F. Ye and D. T. Chiu, *ACS Nano*, 2012, **6**, 5429–5439.
141 K. Pu, A. J. Shuhendler, J. V. Jokerst, J. Mei, S. S. Gambhir, Z. Bao and J. Rao, *Nat. Nanotechnol.*, 2014, **9**, 233–239.
142 Y. Q. Yang, Y. C. Yang, M. H. Liu and Y. H. Chan, *Anal. Chem.*, 2020, **92**, 1493–1501.

143 C. C. Fang, C. C. Chou, Y. Q. Yang, T. Wei-Kai, Y. T. Wang and Y. H. Chan, *Anal. Chem.*, 2018, **90**, 2134–2140.
144 H. Y. Liu, P. J. Wu, S. Y. Kuo, C. P. Chen, E. H. Chang, C. Y. Wu and Y. H. Chan, *J. Am. Chem. Soc.*, 2015, **137**, 10420–10429.
145 Y. W. More, S. D. Padghan, R. S. Bhosale, R. P. Pawar, A. L. Puyad, S. V. Bhosale and S. V. Bhosale, *Sensors*, 2018, **18**, 3433.
146 P. Y. You, F. C. Li, M. H. Liu and Y. H. Chan, *ACS Appl. Mater. Interfaces*, 2019, **11**, 9841–9849.
147 T. M. Allen and P. R. Cullis, *Adv. Drug Delivery Rev.*, 2013, **65**, 36–48.
148 S. Kim and H. D. Sikes, *ACS Appl. Mater. Interfaces*, 2019, **11**, 28469–28477.
149 P. Yingchoncharoen, D. S. Kalinowski and D. R. Richardson, *Pharmacol. Rev.*, 2016, **68**, 701–787.
150 E. Frohnmeyer, N. Tuschel, T. Sitz, C. Hermann, G. T. Dahl, F. Schulz, A. J. Baeumner and M. Fischer, *Analyst*, 2019, **144**, 1840–1849.
151 J. Zheng, X. Hu, Y. Zeng, B. Zhang, Z. Sun, X. Liu, W. Zheng and Y. Chai, *Anal. Chim. Acta*, 2023, **1263**, 341319.
152 Y. Yang, C. Li, H. Shi, T. Chen, Z. Wang and G. Li, *Talanta*, 2019, **192**, 325–330.
153 A. Crintea, A. C. Motofelea, A. S. Sovrea, A. M. Constantin, C. B. Crivii, R. Carpa and A. G. Dutu, *Pharmaceutics*, 2023, **15**, 1406.
154 S. Thakare, A. Shaikh, D. Bodas and V. Gajbhiye, *Colloids Surf., B*, 2022, **209**, 112174.
155 H. Zhang, Z. Lei, R. Tian and Z. Wang, *Talanta*, 2018, **178**, 116–121.
156 M. A. Jafri, S. A. Ansari, M. H. Alqahtani and J. W. Shay, *Genome Med.*, 2016, **8**, 69.
157 S. Cinti, D. Moscone and F. Arduini, *Nat. Protoc.*, 2019, **14**, 2437–2451.
158 L. Rivas, M. Medina-Sanchez, A. de la Escosura-Muniz and A. Merkoci, *Lab Chip*, 2014, **14**, 4406–4414.
159 Q. Tarres, R. Aguado, M. A. Pelach, P. Mutje and M. Delgado-Aguilar, *Nanomaterials*, 2022, **12**, 79.
160 I. Gonzalez, M. Alcala, G. Chinga-Carrasco, F. Vilaseca, S. Boufi and P. Mutje, *Cellulose*, 2014, **21**, 2599–2609.
161 D. Quesada-Gonzalez, C. Stefani, I. Gonzalez, A. de la Escosura-Muniz, N. Domingo, P. Mutje and A. Merkoci, *Biosens. Bioelectron.*, 2019, **141**, 111407.
162 S. Kumar, P. Rai, J. G. Sharma, A. Sharma and B. D. Malhotra, *Adv. Mater. Technol.*, 2016, **1**, 1600056.
163 C. S. Park, C. Lee and O. S. Kwon, *Polymers*, 2016, **8**, 249.
164 S. Kumar, M. Willander, J. G. Sharma and B. D. Malhotra, *J. Mater. Chem. B*, 2015, **3**, 9305–9314.
165 S. Kumar, M. Umar, A. Saifi, S. Kumar, S. Augustine, S. Srivastava and B. D. Malhotra, *Anal. Chim. Acta*, 2019, **1056**, 135–145.
166 F. Bahavarnia, A. Saadati, S. Hassanpour, M. Hasanzadeh, N. Shadjou and A. Hassanzadeh, *Int. J. Biol. Macromol.*, 2019, **138**, 744–754.
167 F. Farschi, A. Saadati and M. Hasanzadeh, *Heliyon*, 2020, **6**, e04327.
168 F. Farshchi, A. Saadati, N. Fathi, M. Hasanzadeh and M. Samiei, *Anal. Methods*, 2021, **13**, 1286–1294.
169 L. Li, Y. Zhang, L. Zhang, S. Ge, H. Liu, N. Ren, M. Yan and J. Yu, *Anal. Chem.*, 2016, **88**, 5369–5377.
170 F. Shi, J. Li, J. Sun, H. Huang, X. Su and Z. Wang, *Talanta*, 2020, **207**, 120341.
171 P. Teengam, W. Siangproh, A. Tuantranont, C. S. Henry, T. Vilaivan and O. Chailapakul, *Anal. Chim. Acta*, 2017, **952**, 32–40.
172 G. Sun, H. Yang, Y. Zhang, J. Yu, S. Ge, M. Yan and X. Song, *Biosens. Bioelectron.*, 2015, **74**, 823–829.
173 W. Zhou, H. Tavakoli, L. Ma, C. Bautista and X. Li, in *Multidisciplinary Microfluidic and Nanofluidic Lab-on-a-chip*, ed. X. Li, C. Yang and P. C. H. Li, Elsevier, Amsterdam, 2022, pp. 325–360, DOI: 10.1016/B978-0-444-59432-7.00009-1.
174 G. Fu, X. Li, W. Wang and R. Hou, *Biosens. Bioelectron.*, 2020, **170**, 112646.
175 H. Torul, H. Ciftci, D. Cetin, Z. Suludere, I. H. Boyaci and U. Tamer, *Anal. Bioanal. Chem.*, 2015, **407**, 8243–8251.
176 S. K. Arya, P. Zhurauski, P. Jolly, M. R. Batistuti, M. Mulato and P. Estrela, *Biosens. Bioelectron.*, 2018, **102**, 106–112.
177 A. Chamorro-Garcia, A. de la Escosura-Muniz, M. Espinosa-Castaneda, C. J. Rodriguez-Hernandez, C. de Torres and A. Merkoci, *Nanomedicine*, 2016, **12**, 53–61.
178 G. Liu, A. S. Gurung and W. Qiu, *Molecules*, 2019, **24**, 756.
179 X. Zhang and Q. Long, *Medicine*, 2017, **96**, e6694.
180 M. Bialkower, H. McLiesh, C. A. Manderson, R. F. Tabor and G. Garnier, *Analyst*, 2019, **144**, 4848–4857.
181 D. C. Christodouleas, B. Kaur and P. Chorti, *ACS Cent. Sci.*, 2018, **4**, 1600–1616.
182 C. M. Oliveira, L. W. Musselwhite, N. de Paula Pantano, F. L. Vazquez, J. S. Smith, J. Schweizer, M. Belmares, J. C. Possati-Resende, M. A. Vieira, A. Longatto-Filho and J. Fregnani, *PLoS One*, 2020, **15**, e0232105.
183 C. Bax, B. J. Lotesoriere, S. Sironi and L. Capelli, *Cancers*, 2019, **11**, 1244.
184 A. D. Warren, G. A. Kwong, D. K. Wood, K. Y. Lin and S. N. Bhatia, *Proc. Natl. Acad. Sci. U. S. A.*, 2014, **111**, 3671–3676.
185 J. Delanghe and M. Speeckaert, *Biochem. Med.*, 2014, **24**, 89–104.
186 S. Kumar, S. Kumar, S. Tiwari, S. Srivastava, M. Srivastava, B. K. Yadav, S. Kumar, T. T. Tran, A. K. Dewan, A. Mulchandani, J. G. Sharma, S. Maji and B. D. Malhotra, *Adv. Sci.*, 2015, **2**, 1500048.
187 S. Aziz, S. S. Ahmed, A. Ali, F. A. Khan, G. Zulfiqar, J. Iqbal, A. A. Khan and M. Shoaib, *Cancer Invest.*, 2015, **33**, 318–328.
188 P. K. Mankapure, S. R. Barpande, J. D. Bhavthankar and M. Mandale, *J. Appl. Oral Sci.*, 2015, **23**, 491–496.
189 Q. Wang, P. Gao, X. Wang and Y. Duan, *Clin. Chim. Acta*, 2014, **427**, 79–85.
190 E. J. Franzmann and M. J. Donovan, *Expert Rev. Mol. Diagn.*, 2018, **18**, 837–844.
191 S. Kumar, J. G. Sharma, S. Maji and B. D. Malhotra, *RSC Adv.*, 2016, **6**, 77037–77046.
192 S. Prasad, A. K. Tyagi and B. B. Aggarwal, *Exp. Biol. Med.*, 2016, **241**, 783–799.
193 N. M. Rodriguez, W. S. Wong, L. Liu, R. Dewar and C. M. Klapperich, *Lab Chip*, 2016, **16**, 753–763.

194 X. Gu, J. Q. Xue, S. J. Han, S. Y. Qian and W. H. Zhang, *Cancer Biomarkers*, 2016, **16**, 395–403.
195 R. Hamam, A. M. Ali, K. A. Alsaleh, M. Kassem, M. Alfayez, A. Aldahmash and N. M. Alajez, *Sci. Rep.*, 2016, **6**, 25997.
196 D. Huo, W. M. Clayton, T. F. Yoshimatsu, J. Chen and O. I. Olopade, *Oncotarget*, 2016, **7**, 55231–55248.
197 M. Li, X. Zou, T. Xia, T. Wang, P. Liu, X. Zhou, S. Wang and W. Zhu, *Cancer Med.*, 2019, **8**, 7006–7017.
198 N. Satomi-Tsushita, A. Shimomura, J. Matsuzaki, Y. Yamamoto, J. Kawauchi, S. Takizawa, Y. Aoki, H. Sakamoto, K. Kato, C. Shimizu, T. Ochiya and K. Tamura, *PLoS One*, 2019, **14**, e0222024.
199 M. Swellam, R. F. K. Zahran, H. Abo El-Sadat Taha, N. El-Khazragy and C. Abdel-Malak, *Arch. Physiol. Biochem.*, 2019, **125**, 456–464.
200 C. Yan, J. Hu, Y. Yang, H. Hu, D. Zhou, M. Ma and N. Xu, *Mol. Med. Rep.*, 2019, **20**, 3991–4002.
201 X. Yu, J. Liang, J. Xu, X. Li, S. Xing, H. Li, W. Liu, D. Liu, J. Xu, L. Huang and H. Du, *J. Breast Cancer*, 2018, **21**, 363–370.
202 Z. Zeng, X. Chen, D. Zhu, Z. Luo and M. Yang, *Yonsei Med. J.*, 2017, **58**, 697–702.
203 X. Zou, M. Li, Z. Huang, X. Zhou, Q. Liu, T. Xia and W. Zhu, *Gene*, 2020, **722**, 144104.
204 T. Aiso, K. Ohtsuka, M. Ueda, S. Karita, T. Yokoyama, S. Takata, N. Matsuki, H. Kondo, H. Takizawa, A. A. Okada, T. Watanabe and H. Ohnishi, *Oncol. Lett.*, 2018, **16**, 6643–6651.
205 L. L. Li, L. L. Qu, H. J. Fu, X. F. Zheng, C. H. Tang, X. Y. Li, J. Chen, W. X. Wang, S. X. Yang, L. Wang, G. H. Zhao, P. P. Lv, M. Zhang, Y. Y. Lei, H. F. Qin, H. Wang, H. J. Gao and X. Q. Liu, *Oncotarget*, 2017, **8**, 45399–45414.
206 M. Sromek, M. Glogowski, M. Chechlinska, M. Kulinczak, L. Szafron, K. Zakrzewska, J. Owczarek, P. Wisniewski, R. Wlodarczyk, L. Talarek, M. Turski and J. K. Siwicki, *Cell. Oncol.*, 2017, **40**, 529–536.
207 Y. Sun, H. Mei, C. Xu, H. Tang and W. Wei, *Pathol., Res. Pract.*, 2018, **214**, 119–125.
208 W. Z. Switlik, M. S. Karbownik, M. Suwalski, J. Kozak and J. Szemraj, *Genet. Test. Mol. Biomarkers*, 2019, **23**, 353–358.
209 L. Wu, B. Hu, B. Zhao, Y. Liu, Y. Yang, L. Zhang and J. Chen, *Oncotarget*, 2017, **8**, 42173–42188.
210 H. J. Yan, J. Y. Ma, L. Wang and W. Gu, *Med. Sci. Monit.*, 2015, **21**, 722–726.
211 X. Yang, Q. Zhang, M. Zhang, W. Su, Z. Wang, Y. Li, J. Zhang, D. G. Beer, S. Yang and G. Chen, *Int. J. Biol. Sci.*, 2019, **15**, 1712–1722.
212 Y. Yang, K. Chen, Y. Zhou, Z. Hu, S. Chen and Y. Huang, *OncoTargets Ther.*, 2018, **11**, 587–597.
213 Y. Zhao, *Int. J. Clin. Exp. Pathol.*, 2018, **11**, 2597–2604.
214 X. Zhou, W. Wen, X. Shan, W. Zhu, J. Xu, R. Guo, W. Cheng, F. Wang, L. W. Qi, Y. Chen, Z. Huang, T. Wang, D. Zhu, P. Liu and Y. Shu, *Oncotarget*, 2017, **8**, 6513–6525.
215 Y. Wang, C. Zhang, P. Zhang, G. Guo, T. Jiang, X. Zhao, J. Jiang, X. Huang, H. Tong and Y. Tian, *Cancer Med.*, 2018, **7**, 1670–1679.
216 A. Weis, L. Marquart, D. A. Calvopina, B. Genz, G. A. Ramm and R. Skoien, *Int. J. Mol. Sci.*, 2019, **20**, 864.
217 A. Habieb, M. Matboli, H. El-Tayeb and F. El-Asmar, *Mol. Biol. Rep.*, 2019, **46**, 4581–4590.
218 E. G. E. El-Ahwany, L. Mourad, M. M. K. Zoheiry, H. Abu-Taleb, M. Hassan, R. Atta, M. Hassanien and S. Zada, *Arch. Med. Sci.*, 2019, **15**, 1454–1461.
219 S. A. Dhayat, A. Husing, N. Senninger, H. H. Schmidt, J. Haier, H. Wolters and I. Kabar, *PLoS One*, 2015, **10**, e0140066.
220 S. Mummareddy, S. Pradhan, A. K. Narasimhan and A. Natarajan, *Biosensors*, 2021, **11**, 500.
221 I. E. Tothill, *Semin. Cell Dev. Biol.*, 2009, **20**, 55–62.
222 H. Khan, M. R. Shah, J. Barek and M. I. Malik, *TrAC, Trends Anal. Chem.*, 2023, **158**, 116813.
223 T. H. Chen, C. T. Chiu, C. Lee, Y. Y. Chu, H. T. Cheng, J. T. Hsu, R. C. Wu, T. S. Yeh and K. H. Lin, *Dig. Dis. Sci.*, 2018, **63**, 2301–2308.
224 S. S. Emami, R. Nekouian, A. Akbari, A. Faraji, V. Abbasi and S. Agah, *J. Cancer Res. Ther.*, 2019, **15**, 115–119.
225 T. Imamura, S. Komatsu, D. Ichikawa, M. Miyamae, W. Okajima, T. Ohashi, J. Kiuchi, K. Nishibeppu, T. Kosuga, H. Konishi, A. Shiozaki, K. Okamoto, H. Fujiwara and E. Otsuji, *Oncotarget*, 2017, **8**, 106538–106550.
226 H. Imaoka, Y. Toiyama, M. Okigami, H. Yasuda, S. Saigusa, M. Ohi, K. Tanaka, Y. Inoue, Y. Mohri and M. Kusunoki, *Gastric Cancer*, 2016, **19**, 744–753.
227 X. Jiang, W. Wang, Y. Yang, L. Du, X. Yang, L. Wang, G. Zheng, W. Duan, R. Wang, X. Zhang, L. Wang, X. Chen and C. Wang, *Oncotarget*, 2017, **8**, 65132–65142.
228 M. Y. Song, K. F. Pan, H. J. Su, L. Zhang, J. L. Ma, J. Y. Li, Y. Yuasa, D. Kang, Y. S. Kim and W. C. You, *PLoS One*, 2012, **7**, e33608.
229 M. M. Tsai, C. S. Wang, C. Y. Tsai, C. G. Huang, K. F. Lee, H. W. Huang, Y. H. Lin, H. C. Chi, L. M. Kuo, P. H. Lu and K. H. Lin, *Eur. J. Cancer*, 2016, **64**, 137–148.
230 N. Wang, L. Wang, Y. Yang, L. Gong, B. Xiao and X. Liu, *Biochem. Biophys. Res. Commun.*, 2017, **493**, 1322–1328.
231 G. Zhao, T. Jiang, Y. Liu, G. Huai, C. Lan, G. Li, G. Jia, K. Wang and M. Yang, *BMC Cancer*, 2018, **18**, 676.
232 X. Zhou, W. Wen, J. Zhu, Z. Huang, L. Zhang, H. Zhang, L. W. Qi, X. Shan, T. Wang, W. Cheng, D. Zhu, Y. Yin, Y. Chen, W. Zhu, Y. Shu and P. Liu, *Oncotarget*, 2017, **8**, 34468–34480.
233 E. Bilegsaikhan, H. N. Liu, X. Z. Shen and T. T. Liu, *J. Dig. Dis.*, 2018, **19**, 404–410.
234 H. Cheng, L. Zhang, D. E. Cogdell, H. Zheng, A. J. Schetter, M. Nykter, C. C. Harris, K. Chen, S. R. Hamilton and W. Zhang, *PLoS One*, 2011, **6**, e17745.
235 X. Liu, X. Xu, B. Pan, B. He, X. Chen, K. Zeng, M. Xu, Y. Pan, H. Sun, T. Xu, X. Hu and S. Wang, *J. Cancer*, 2019, **10**, 43–50.
236 L. Min, S. Zhu, L. Chen, X. Liu, R. Wei, L. Zhao, Y. Yang, Z. Zhang, G. Kong, P. Li and S. Zhang, *J. Extracell. Vesicles*, 2019, **8**, 1643670.

237 Y. Tan, J. J. Lin, X. Yang, D. M. Gou, L. Fu, F. R. Li and X. F. Yu, *Cancer Epidemiol.*, 2019, **60**, 67–76.
238 M. L. Wikberg, R. Myte, R. Palmqvist, B. van Guelpen and I. Ljuslinder, *Cancer Med.*, 2018, **7**, 1697–1705.
239 H. Zhang, M. Zhu, X. Shan, X. Zhou, T. Wang, J. Zhang, J. Tao, W. Cheng, G. Chen, J. Li, P. Liu, Q. Wang and W. Zhu, *Gene*, 2019, **687**, 246–254.
240 G. Zou, R. Wang and M. Wang, *Cancer Biomarkers*, 2019, **25**, 11–18.
241 Q. Chen, L. Yang, Y. Xiao, J. Zhu and Z. Li, *Med. Oncol.*, 2014, **31**, 225.
242 P. Karasek, N. Gablo, J. Hlavsa, I. Kiss, P. Vychytilova-Faltejskova, M. Hermanova, Z. Kala, O. Slaby and V. Prochazka, *Cancer Genomics Proteomics*, 2018, **15**, 321–327.
243 X. Lai, M. Wang, S. D. McElyea, S. Sherman, M. House and M. Korc, *Cancer Lett.*, 2017, **393**, 86–93.
244 F. Li, J. W. Xu, L. Wang, H. Liu, Y. Yan and S. Y. Hu, *Artif. Cells, Nanomed., Biotechnol.*, 2018, **46**, 482–487.
245 K. Qu, X. Zhang, T. Lin, T. Liu, Z. Wang, S. Liu, L. Zhou, J. Wei, H. Chang, K. Li, Z. Wang, C. Liu and Z. Wu, *Sci. Rep.*, 2017, **7**, 1692.
246 P. Skrha, A. Horinek, E. Pazourkova, J. Hajer, P. Fric, J. Skrha and M. Andel, *Pancreatology*, 2016, **16**, 839–843.
247 A. J. Stroese, H. Ullerich, G. Koehler, V. Raetzel, N. Senninger and S. A. Dhayat, *J. Cancer Res. Clin. Oncol.*, 2018, **144**, 2377–2390.
248 X. Zou, J. Wei, Z. Huang, X. Zhou, Z. Lu, W. Zhu and Y. Miao, *Cancer Med.*, 2019, **8**, 2810–2822.
249 T. Kim and C. M. Croce, *Exp. Mol. Med.*, 2023, **55**, 1314–1321.
250 H. Lin, X. Shi, H. Li, J. Hui, R. Liu, Z. Chen, Y. Lu and W. Tan, *BMC Cancer*, 2021, **21**, 1293.
251 J. T. Lin and K. W. Tsai, *Int. J. Mol. Sci.*, 2021, **22**, 4278.
252 D. Coradduzza, T. Solinas, F. Balzano, N. Culeddu, N. Rossi, S. Cruciani, E. Azara, M. Maioli, A. Zinellu, M. R. De Miglio, M. Madonia, M. Falchi and C. Carru, *J. Mol. Diagn.*, 2022, **24**, 1171–1180.
253 X. Fan, X. Zou, C. Liu, W. Cheng, S. Zhang, X. Geng and W. Zhu, *Biosci. Rep.*, 2021, **41**, BSR20210111.
254 C. Huang, Y. Sun, S. Ma, A. S. Vadamootoo, L. Wang and C. Jin, *Pathol., Res. Pract.*, 2019, **215**, 152411.
255 L. Zhou, X. Ma, J. Yue, T. Chen, X. Y. Wang, Z. W. Wang, J. Pan and Y. Lin, *Cancer Biomarkers*, 2018, **23**, 561–567.
256 Z. S. Yao, C. Li, D. Liang, X. B. Jiang, J. J. Tang, L. Q. Ye, K. Yuan, H. Ren, Z. D. Yang, D. X. Jin, S. C. Zhang, J. Y. Ding, Y. C. Tang, J. X. Xu, K. Chen, W. X. Xie, D. Q. Guo and J. C. Cui, *Cancer Biomarkers*, 2018, **22**, 127–133.
257 D. Ouyang, N. Ye, Y. Jiang, Y. Wang, L. Hu, S. Chao, M. Yarmush, M. Tuner, Y. Li and B. Tang, *Biomed. Microdevices*, 2023, **26**, 3.
258 J. Prada-Arismendy, J. C. Arroyave and S. Röthlisberger, *Blood Rev.*, 2017, **31**, 63–76.
259 J. Zhao and Y. Lin, *Front. Oncol.*, 2023, **13**, 1132628.
260 H. Sareen, Y. Ma, T. M. Becker, T. L. Roberts, P. de Souza and B. Powter, *Int. J. Mol. Sci.*, 2022, **23**, 8835.
261 S. Tamai, T. Ichinose and M. Nakada, *Brain Tumor Pathol.*, 2023, **40**, 66–77.
262 Y. Xiao, L. Zhang, Z. Song, C. Guo, J. Zhu, Z. Li and S. Zhu, *Med. Sci. Monit.*, 2016, **22**, 855–862.
263 F. Zhi, N. Shao, R. Wang, D. Deng, L. Xue, Q. Wang, Y. Zhang, Y. Shi, X. Xia, S. Wang, Q. Lan and Y. Yang, *Neuro-Oncology*, 2015, **17**, 383–391.
264 T. Zhang, F. Ding, Y. Yang, G. Zhao, C. Zhang, R. Wang and X. Huang, *Biosensors*, 2022, **12**, 485.
265 J. Q. Sheng, S. R. Li, Z. T. Wu, C. H. Xia, X. Wu, J. Chen and J. Rao, *Cancer Epidemiol., Biomarkers Prev.*, 2009, **18**, 2182–2185.
266 M. Oliveira-Rodriguez, S. Lopez-Cobo, H. T. Reyburn, A. Costa-Garcia, S. Lopez-Martin, M. Yanez-Mo, E. Cernuda-Morollon, A. Paschen, M. Vales-Gomez and M. C. Blanco-Lopez, *J. Extracell. Vesicles*, 2016, **5**, 31803.
267 G. Liu, X. Mao, J. A. Phillips, H. Xu, W. Tan and L. Zeng, *Anal. Chem.*, 2009, **81**, 10013–10018.
268 A. Javani, F. Javadi-Zarnaghi and M. J. Rasaee, *Anal. Biochem.*, 2017, **537**, 99–105.
269 P. Preechakasedkit, W. Siangproh, N. Khongchareonporn, N. Ngamrojanavanich and O. Chailapakul, *Biosens. Bioelectron.*, 2018, **102**, 27–32.
270 K. Baryeh, S. Takalkar, M. Lund and G. D. Liu, *J. Pharm. Biomed. Anal.*, 2017, **146**, 285–291.
271 A. S. Ghrera, C. M. Pandey, M. A. Ali and B. D. Malhotra, *Appl. Phys. Lett.*, 2015, **106**, 193703.
272 J. V. Jokerst, A. Raamanathan, N. Christodoulides, P. N. Floriano, A. A. Pollard, G. W. Simmons, J. Wong, C. Gage, W. B. Furmaga, S. W. Redding and J. T. McDevitt, *Biosens. Bioelectron.*, 2009, **24**, 3622–3629.
273 D. Y. Zhang, Y. L. Wang, X. Y. Jin, Q. Xiao and S. Huang, *Analyst*, 2022, **147**, 2412–2424.
274 B. Salim, M. V. Athira, A. Kandaswamy, M. Vijayakumar, T. Saravanan and T. Sairam, *Biomed. Microdevices*, 2017, **19**, 89.
275 Y. Wu, P. Xue, Y. Kang and K. M. Hui, *Anal. Chem.*, 2013, **85**, 8661–8668.
276 W. Li, M. Li, S. Ge, M. Yan, J. Huang and J. Yu, *Anal. Chim. Acta*, 2013, **767**, 66–74.
277 T. H. Ulep, R. Zenhausern, A. Gonzales, D. S. Knoff, P. A. Lengerke Diaz, J. E. Castro and J. Y. Yoon, *Biosens. Bioelectron.*, 2020, **153**, 112042.
278 A. Saadati, S. Hassanpour, F. Bahavarnia and M. Hasanzadeh, *Anal. Methods*, 2020, **12**, 1639–1649.
279 Y. Fan, S. Shi, J. Ma and Y. Guo, *Biosens. Bioelectron.*, 2019, **135**, 1–7.
280 S. Kumar, S. Kumar, S. Srivastava, B. K. Yadav, S. H. Lee, J. G. Sharma, D. C. Doval and B. D. Malhotra, *Biosens. Bioelectron.*, 2015, **73**, 114–122.
281 A. T. Singh, D. Lantigua, A. Meka, S. Taing, M. Pandher and G. Camci-Unal, *Sensors*, 2018, **18**, 2838.

282 C. Desmet, C. A. Marquette, L. J. Blum and B. Doumeche, *Biosens. Bioelectron.*, 2016, **76**, 145–163.
283 Y. Q. Wu, Z. W. Sun, F. C. Gao, Y. D. Wang and Y. Y. Jiang, *Adv. Mater. Technol.*, 2023, **8**, 2300357.
284 M. H. Son, S. W. Park, H. Y. Sagong and Y. K. Jung, *BioChip J.*, 2023, **17**, 44–67.
285 Z. Yu, H. Gong, F. Xue, Y. Zeng, X. Liu and D. Tang, *Anal. Chem.*, 2022, **94**, 13233–13242.
286 S. Lv, Y. Tang, K. Zhang and D. Tang, *Anal. Chem.*, 2018, **90**, 14121–14125.
287 L. Huang, R. Zeng, J. Xu and D. Tang, *Anal. Chem.*, 2022, **94**, 13278–13286.
288 Z. Yu, Y. Tang, G. Cai, R. Ren and D. Tang, *Anal. Chem.*, 2019, **91**, 1222–1226.
289 Z. Yu, H. Gong, Y. Li, J. Xu, J. Zhang, Y. Zeng, X. Liu and D. Tang, *Anal. Chem.*, 2021, **93**, 13389–13397.
290 Z. Yu, H. Gong, J. Xu, Y. Li, Y. Zeng, X. Liu and D. Tang, *Anal. Chem.*, 2022, **94**, 3418–3426.
291 Z. Yu, Q. Lin, H. Gong, M. Li and D. Tang, *Biosens. Bioelectron.*, 2023, **223**, 115028.
292 M. Magiati, A. Sevastou and D. P. Kalogianni, *Microchim. Acta*, 2018, **185**, 314.
293 L. L. Wang, L. P. Zeng, Y. R. Wang, T. T. Chen, W. Q. Chen, G. Y. Chen, C. Y. Li and J. H. Chen, *Sens. Actuators, B*, 2021, **332**, 129471.
294 S. H. Luo, Y. Wu, W. L. Pan, G. Z. Zhong, B. Situ, B. Li, X. Y. Ye, X. J. Jiang, W. B. Li, Y. Zhang, L. Zheng and Q. Wang, *Sens. Actuators, B*, 2023, **374**, 132792.
295 M. Mahmoodpour, B. A. Kiasari, M. Karimi, A. Abroshan, D. Shamshirian, H. Hosseinalizadeh, A. Delavari and H. Mirzei, *Front. Oncol.*, 2023, **13**, 1131435.
296 M. Butler, L. Pongor, Y. T. Su, L. Xi, M. Raffeld, M. Quezado, J. Trepel, K. Aldape, Y. Pommier and J. Wu, *Trends Cancer*, 2020, **6**, 380–391.
297 J. Prada-Arismendy, J. C. Arroyave and S. Rothlisberger, *Blood Rev.*, 2017, **31**, 63–76.
298 K. P. Divya, S. Keerthana, C. Viswanathan and N. Ponpandian, *Microchim. Acta*, 2023, **190**, 116.
299 M. S. Draz, M. Moazeni, M. Venkataramani, H. Lakshminarayanan, E. Saygili, N. K. Lakshminaraasimulu, K. M. Kochehbyoki, M. K. Kanakasabapathy, S. Shabahang, A. Vasan, M. A. Bijarchi, A. Memic and H. Shafiee, *Adv. Funct. Mater.*, 2018, **28**, 1707161.
300 E. R. Kim, C. Joe, R. J. Mitchell and M. B. Gu, *Trends Biotechnol.*, 2023, **41**, 374–395.